TECHNICAL REPORT R-75

ANALYTICAL STUDY OF SOFT LANDINGS ON GAS-FILLED BAGS

By JACK B. ESGAR and WILLIAM C. MORGAN

Lewis Research Center
Cleveland, Ohio

TECHNICAL REPORT R-75

ANALYTICAL STUDY OF SOFT LANDINGS ON GAS-FILLED BAGS

By Jack B. Esgar and William C. Morgan

SUMMARY

An analytical study was conducted to develop a procedure for determining the deceleration characteristics of vehicles landing on gas-filled bags of various arbitrary shapes. The analysis developed is applicable for landing on planetary or lunar surfaces for sinking speeds that are small compared to the sonic velocity of the gas contained within the bag. For relatively high velocities a light gas such as hydrogen or helium should probably be used. A series of calculations was made for four bag shapes for impact on the earth at sea-level conditions for sinking speeds consistent with descent by parachute to determine how deceleration characteristics were influenced by various factors entering the equations.

It was found that gas-filled bags can be used to absorb landing shocks at normal parachute sinking speeds with deceleration and onset rate acceptable for well-supported human beings. From the standpoints of maximum deceleration and required stroke, the vertical cylinder appears to be the best shape studied. Multiple bags should probably be used with all shapes to accept cocked impacts.

A method of controlled gas bleed from the bags is required. The ideal method would be to utilize pressure-actuated orifices of variable area that could maintain constant pressure in the bag. Bags with constant-area orifices of proper size would be satisfactory, but would require a somewhat greater stroke for a given maximum deceleration. It would be possible, however, to utilize bags without bleed during the deceleration process, but the bags would have to be rapidly deflated at the end of the stroke to eliminate or reduce bounce.

INTRODUCTION

The landing of nonlifting vehicles on the earth, moon, or planets requires some sort of deceleration device at the time of impact to protect the vehicle and its payload. This report presents an analytical study of a variety of gas-filled bag shapes for providing reasonable deceleration rates at impact.

Vehicles that descend from space or from a planet's atmosphere must be protected from damage during landing if the vehicle is to be reused or if the cargo is of a delicate nature, such as instruments or human or animal life. Several deceleration methods or combinations of methods are possible. A common method of descending is to use a lifting vehicle such as an airplane or glider. Other deceleration and landing devices include mechanisms for providing vertical thrust such as obtained from helicopter rotors or retrorockets and atmospheric drag devices such as blunt bodies and parachutes. In the latter category, vertical velocity is not completely dissipated; therefore, some sort of shock absorption device is required at impact. If a water landing is to be made, adequate shock absorption can often be obtained by proper contouring of the impacting surface so that reasonable deceleration rates can be obtained by water displacement (ref. 1). If, however, impact is to be made on a hard surface such as land, the kinetic energy of the descending body must generally be absorbed within a portion of the body's structure or contents in order to bring the body to rest. In order to keep deceleration rates to reasonable values, this kinetic energy must be absorbed over some distance. This distance will be proportional to the square of the velocity for a given deceleration. Possible methods of absorbing this energy include heat generation within a collapsible portion of the structure (refs. 2 and 3) or compression and/or acceleration of captive gases within a pneumatic bag or cylinder.

Landing on gas-filled bags has been investigated and used for parachute recovery of unpiloted aircraft and missiles and equipment delivery by parachute (refs. 4 to 8). It seems to be a promising deceleration method for landing on planets. The bags could be filled with gas from

the planet's atmosphere during descent which would provide an additional weight saving. For a lunar landing, gas for filling the bag would have to be carried along in the landing vehicle. Analysis of gas-filled spheres landing at high speed on the moon is discussed in references 9 and 10.

Previous investigations of vehicles descending on top of gas-filled bags have been primarily experimental or directed towards one specific application and have not presented a sound analytical basis for a generalized study of the deceleration characteristics. Since this method offers promise for deceleration of bodies at impact, an analytical investigation was conducted to determine the deceleration characteristics of vehicles landing on a variety of gas-filled bag shapes with and without gas bleed during the impact stroke. (Stroke is defined as the travel or movement of vehicle after the bag first impacts.) Bag shapes studied included vertical cylinders, horizontal cylinders, spheres, and hemispheres. Bleed rates considered were those that would maintain a constant gas pressure in the bag and those that would occur through an orifice of a constant diameter. Typical results are presented for ranges of impact velocity, bag height, ratio of body mass to bag volume, bag configuration, initial bag pressure, and bleed rates.

DISCUSSION OF PROBLEM

This report is concerned primarily with the thermodynamics of landing on gas-filled bags. From such an analysis it is possible to determine how various factors such as mass, bag height, bag shape, bag volume, initial pressure, and initial velocity affect deceleration, deceleration onset rate (rate of change of deceleration with time), pressure buildup, and variation of velocity with stroke. Other factors must also be considered in the design. Although these factors are not treated comprehensively, some discussion is warranted so that the reader can have a better understanding of the general problem. In this light, he should be more capable of evaluating and applying the results of this analytical study. Some of the problems requiring consideration are strength, durability, storage, weight, inflation, and bleed methods for the bag, and stability of the vehicle during descent prior to impact, during the deceleration process, and during any rebound that may result from the compressed gas within the bag.

The deceleration during landing can be made arbitrarily small by employing a tall, slender bag that gradually decelerates the vehicle during compression of the bag's great height. Such a bag would not have the requisite stability. It might buckle as would a slender column under slight misalinement of forces, and it would be prone to tip over because of side drift or cocking at impact. Highly stable bags will generally be short and have a large area in contact with the landing surface. These characteristics are diametrically opposed to the requirements for low deceleration. Any given design of landing bags will thus be a compromise between the demands for stability and low deceleration.

In the design of a landing-bag system, the vehicle and its payload must have the ability to withstand some given deceleration and deceleration onset, and the system must stay within these limitations. It must also accept reasonable variations in the landing surface, lateral speed, and cocking at impact. Rebounding appears to jeopardize vehicle stability and should be minimized or avoided. A good landing-bag system would decelerate the vehicle in the following manner: From the first moment of impact deceleration would rise at a high, but acceptable, rate until a limit on deceleration had been reached. Deceleration would then remain near this limiting level until the vehicle had essentially been brought to rest and was near the ground surface. The captive gas in the bags should be released at this point. Rupturing might be desirable. The use of high and nearly constant deceleration would reduce the distance for deceleration (herein called stroke) to the smallest value within the vehicle's strength limitations, and by use of short, large-surface contact bags it would thereby somewhat relieve the problem of obtaining impacting stability.

The type of landing described will require bleeding of gas from the bag during the deceleration process at a prescribed, variable rate. Possible methods of controlling this rate include a variable-bleed orifice area where the area could be varied by means of a pressure-actuated device or by a contoured metering rod in the orifice that would be actuated by stroke. The metering rod concept could be very similar to that utilized in aircraft landing gear.

Stability prior to impact can be improved by using multiple parachutes to reduce swinging. Stability after impact can be improved by making use of a multiple-bag system. Such a system has the advantage of having bags located to accept off-design impact orientations. In addition, the gas shifting that can reduce the support in cocked landings of a large single bag can be essentially eliminated in multiple bags. For the same stress level in the bag material, there is no weight penalty associated with the use of multiple bags having the same total volume as a single larger bag.

Further discussion of some of the factors affecting bag design can be found in references 2 to 8. In the remainder of this report the analysis will only be concerned with the deceleration characteristics of vehicles descending vertically and impacting on a flat surface.

ANALYSIS

ASSUMPTIONS AND BASIC EQUATIONS

In making the analysis, the following assumptions were made:

(1) The gas bag is flexible, but inelastic (nonstretchable).

(2) Gas pressure forces and aerodynamic drag (mostly parachute) are only forces causing mass to decelerate. Friction, bag bending resistance, and parachute shroud line elasticity are neglected.

(3) Compression of gas inside bag occurs adiabatically.

(4) Vehicle is descending vertically.

(5) For cases with aerodynamic drag the drag equals weight at moment of bag impact.

(6) The mass of the gas in the bag is negligible compared with the overall vehicle mass.

For a vehicle descending in a vertical direction on a gas bag as illustrated in figure 1, the following force balance can be written using the symbols given in appendix A:

$$ma+mg+p_0A=pA+\frac{\rho_0 U^2}{2g}C_DA_D \qquad (1)$$

The physical explanations of the terms in the equation are as follows:

First term: Downward force due to deceleration of vehicle

Second term: Downward force due to gravity

Third term: Net downward force due to atmospheric pressure

Fourth term: Upward force due to pressure within bag

Fifth term: Upward force due to aerodynamic drag

In this analysis it will be convenient to express the pressure of the gas in the bag as a function of the volume by the expression

$$p=C_1v^{-n} \qquad (2)$$

where

$$n\leq\gamma$$

For adiabatic compression with no gas bleed from the bag, $n=\gamma$. For leakage at a controlled rate such that the pressure is constant, $n=0$. For other leakage rates n may be either positive or negative, but it is always less than γ. For these cases n will probably also vary with the distance x shown in figure 1. For cases where n is a variable, closed-form solutions were not obtained.

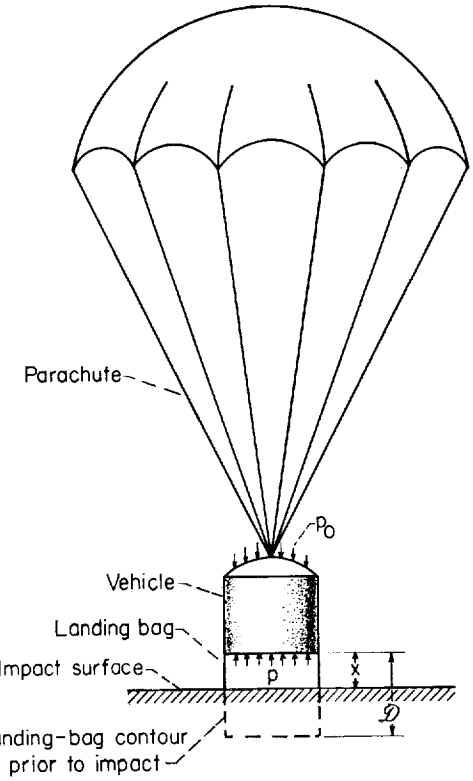

FIGURE 1.- Conditions during impact of parachute-borne vehicle fitted with landing bag.

A general, closed-form solution was not found to relate the instantaneous velocity with stroke for the case where the effects of aerodynamic drag are included. In the ANALYSIS section, therefore, velocity equations will first be derived in which the effects of aerodynamic drag are neglected. The effects of drag on velocity will be considered subsequently for special cases. The effects of drag will always be considered in calculating deceleration and deceleration onset.

In the derivation of the equations in this analytical study, the terms are arranged in a manner convenient for analyzing deceleration on a planet where there is an atmosphere. For a lunar landing where the atmospheric pressure p_0 is zero, some of the terms in the equations as derived become indeterminate. These equations are rearranged in a form suitable for making calculations for lunar landings and are presented in appendix B.

VELOCITY EQUATIONS WITH AERODYNAMIC DRAG NEGLECTED

In most cases the error involved in neglecting effects of aerodynamic drag, even with a parachute, will be small because the drag force is small compared to the gas pressure forces. This is particularly true after the body starts to slow down because the aerodynamic drag is proportional to the square of the sinking speed. By neglecting the term for aerodynamic drag, the equation for the force balance can be handled in a generalized manner for a variety of bag shapes.

By noting that

$$U=-\frac{dx}{dt} \tag{3}$$

and

$$a=-\frac{dU}{dt}=\frac{U\,dU}{dx} \tag{4}$$

and neglecting the term for aerodynamic drag, equation (1) becomes

$$mU\,dU+mg\,dx+p_0A\,dx=pA\,dx \tag{5}$$

It will be convenient to write equation (5) in the form

$$mU\,dU+mg\,dx+p_0v_t\,d\psi=p_iv_i\psi^{-n}\,d\psi \tag{6}$$

where ψ is a dimensionless volume and, from equation (2),

$$p=p_i\left(\frac{v_i}{v}\right)^n=p_i\psi^{-n} \tag{7}$$

Table I gives relations for volumes and areas for the geometries shown in figure 2. The relations are derived in appendix C. By using expressions in table I, equations (5) and (6) can be shown to be equal.

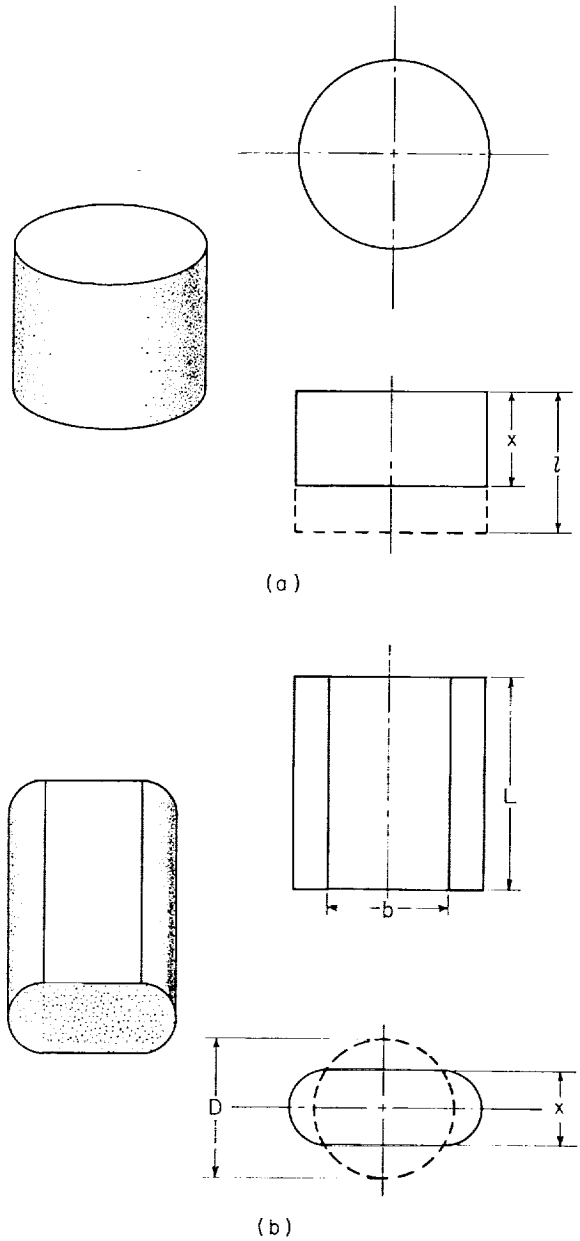

(a) Vertical cylinder.
(b) Horizontal cylinder.

FIGURE 2.—Landing-bag shapes considered in analysis.

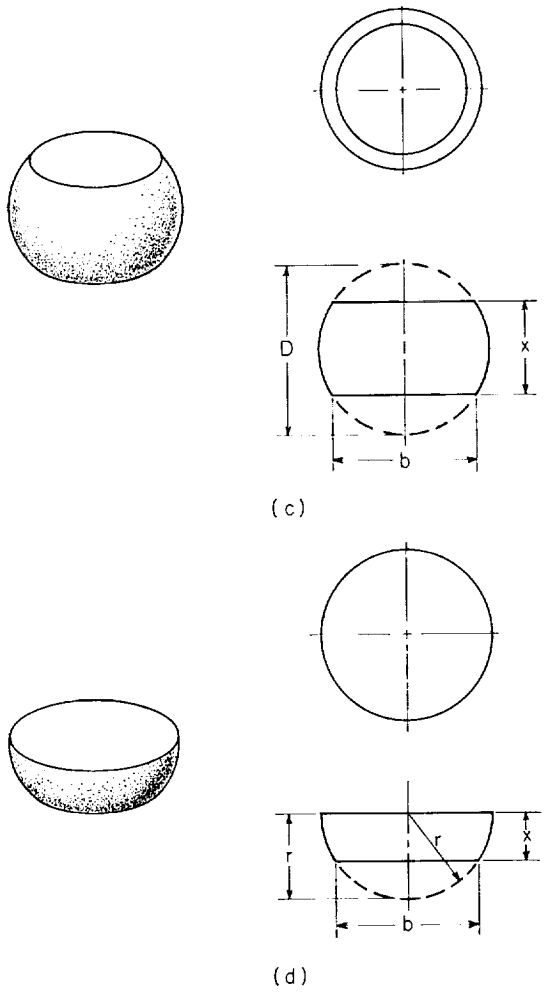

(c) Sphere.
(d) Hemisphere.

FIGURE 2.—Concluded. Landing-bag shapes considered in analysis.

Integration of equation (6) between the limits $\mathscr{D}$ to x and U_i to U with constant n results in

$$\left(\frac{U}{U_i}\right)^2=1+\frac{2v_ip_0}{mU_i^2}\left[1+\beta\left(1-\frac{x}{\mathscr{D}}\right)-\frac{1}{n-1}\frac{p_i}{p_0}(\psi^{1-n}-1)-\psi\right] \tag{8}$$

which gives the velocity of the decelerating body as a function of x and the initial conditions at point of impact. Table I gives expressions for β and ψ for the various bag shapes considered.

Equation (8) is valid for the case where the bag is fully inflated at the beginning of the deceleration process. For the case where the bag is either not fully inflated or partially compressed, the initial bag height in this state is designated as x^* and the velocity at this position as U^*. Integration of equation (6) between the limits x^* to x and U^* to U results in

$$\left(\frac{U}{U^*}\right)^2=1+\frac{2v_ip_0}{mU^{*2}}\left\{\frac{mgx^*}{v_ip_0}\left(1-\frac{x}{x^*}\right)+\frac{(\psi^*)^n}{n-1}\frac{p^*}{p}[(\psi^*)^{1-n}-\psi^{1-n}]+\psi^*-\psi\right\} \tag{9}$$

where ψ^* is evaluated from table I by substituting x^* for x in the expression for ψ.

For the special case where $n=1$, equations (8) and (9) take the forms

$$\left(\frac{U}{U_i}\right)^2=1+\frac{2v_ip_0}{mU_i^2}\left[1+\beta\left(1-\frac{x}{\mathscr{D}}\right)-\frac{p_i}{p_0}\ln\frac{1}{\psi}-\psi\right] \tag{8a}$$

$$\left(\frac{U}{U^*}\right)^2=1+\frac{2v_ip_0}{mU^{*2}}\left\{\frac{mgx^*}{v_ip_0}\left(1-\frac{x}{x^*}\right)+\psi^*\frac{p^*}{p_0}\left(\ln\frac{1}{\psi^*}-\ln\frac{1}{\psi}\right)+\psi^*-\psi\right\} \tag{9a}$$

EQUATIONS WITH AERODYNAMIC DRAG CONSIDERED

Deceleration.—For constant descent velocity just prior to impact, the aerodynamic drag equals the weight of the descending vehicle. By assuming the drag coefficient is independent of velocity, the drag term in equation (1) can be written:

$$\frac{\rho_0U^2}{2g}C_DA_D=mg\left(\frac{U}{U_i}\right)^2 \tag{10}$$

The deceleration can be obtained as a function of x by combining equations (1), (7), and (10) to obtain

$$\frac{a}{g}=\frac{Ap_0}{mg}\left(\frac{p_i}{p_0}\psi^{-n}-1\right)+\left(\frac{U}{U_i}\right)^2-1 \tag{11}$$

which can be written

$$\frac{a}{g}=\frac{\epsilon}{\beta}\left(\frac{p_i}{p_0}\psi^{-n}-1\right)+\left(\frac{U}{U_i}\right)^2-1 \tag{12}$$

where the values of ϵ, β, and ψ are given in table I for various bag shapes. In a corresponding manner, the deceleration for the case where the bag is not fully inflated or is partially compressed

at the beginning of the deceleration process results in

$$\frac{a}{g}=\frac{\epsilon}{\beta}\left[\frac{p^*}{p_0}\left(\frac{\psi}{\psi^*}\right)^{-n}-1\right]+\left(\frac{U}{U^*}\frac{U^*}{U_i}\right)^2-1 \quad (12a)$$

The term U^*/U_i will be equal to unity if the deceleration begins with a partially deflated bag. There are some cases, however, where the vehicle may be decelerated partially so that $U^*\neq U_i$, and then the term will be needed. The velocity U_i corresponds to the equilibrium sinking speed of the vehicle using a parachute or other aerodynamic drag device.

If there is no aerodynamic drag, the velocity terms are omitted from equations (12) and (12a).

Deceleration onset rate.—The rate of deceleration onset is also of importance. Deceleration onset rate is defined as the rate of change of deceleration with time. This onset rate can be obtained by differentiating equation (12) with respect to time which yields

$$\frac{\dot{a}}{g}=\frac{\dot{\epsilon}}{\beta}\left(\frac{p_i}{p_0}\psi^{-n}-1\right)-\frac{n\epsilon}{\beta}\frac{p_i}{p_0}\psi^{-(n+1)}\dot{\psi}+\frac{2U}{U_i^2}\dot{U} \quad (13)$$

It can be shown that

$$\dot{\psi}=-\frac{U}{\mathscr{D}}\epsilon$$

Then, combining equations (3), (4), and (13) and defining

$$\mu=\frac{\dot{\epsilon}}{U/\mathscr{D}}$$

result in

$$\frac{\dot{a}}{g}=\frac{U}{U_i}\left\{\frac{U_i}{\beta\mathscr{D}}\left[\frac{p_i}{p_0}\psi^{-n}\left(\frac{n\epsilon^2}{\psi}+\mu\right)-\mu\right]-\frac{2g}{U_i}\left(\frac{a}{g}\right)\right\} \quad (14)$$

where the value of the velocity term is obtained from equation (8) and the value of the deceleration term is obtained from equation (12) for the corresponding value of x. The term μ can be shown to be a function of x, and values of μ are given in table I for each bag shape.

In a similar manner, the deceleration onset rate can be found for the case where the bag is not fully inflated at the beginning of the deceleration process by differentiating equation (12a) with the result

$$\frac{\dot{a}}{g}=\frac{U}{U^*}\left\{\frac{U^*}{\beta\mathscr{D}}\left[\frac{p^*}{p_0}\left(\frac{\psi}{\psi^*}\right)^{-n}\left(\frac{n\epsilon^2}{\psi}+\mu\right)-\mu\right]-\frac{2g}{U^*}\left(\frac{U^*}{U_i}\right)^2\left(\frac{a}{g}\right)\right\} \quad (14a)$$

where the value of the velocity term U/U^* is obtained from equation (9) and the value of the deceleration term is obtained from equation (12a).

Approximate velocity.—For vehicles subjected to aerodynamic drag, the velocity calculated by equation (8) will be slightly high. The deceleration calculated by equation (12) will be reasonably accurate even though the value of the velocity term in the equation is evaluated by equation (8), which neglects drag. Small errors in this velocity will have a negligible effect on calculated deceleration. By using the calculated values of deceleration it is possible to obtain more accurate values of velocity in which aerodynamic drag is accounted for. A stepwise procedure is used to calculate the change in velocity over a small increment of stroke Δx based on the average deceleration for Δx. Equation (4) can be written in incremental form

$$\frac{\bar{a}}{g}=\frac{\bar{U}}{g}\frac{\Delta U}{\Delta x}$$

or

$$\left(\frac{a}{g}\right)_{x+\Delta x}+\left(\frac{a}{g}\right)_x=(U_{x+\Delta x}+U_x)\left(\frac{U_{x+\Delta x}-U_x}{g\,\Delta x}\right)=\frac{U_{x+\Delta x}^2-U_x^2}{g\,\Delta x} \quad (15)$$

By a stepwise procedure starting at $x+\Delta x=\mathscr{D}$, the velocity at x can be obtained relative to the velocity at $x+\Delta x$ from equation (15) written in the form

$$\left(\frac{U}{U_i}\right)_x^2=\left(\frac{U}{U_i}\right)_{x+\Delta x}^2-\frac{g\,\Delta x}{U_i^2}\left[\left(\frac{a}{g}\right)_{x+\Delta x}+\left(\frac{a}{g}\right)_x\right] \quad (16)$$

where the values of a/g are obtained from equation (12).

Velocity for vertical cylinder.—The vertical cylinder (axis parallel to direction of descent) was the only bag shape considered for a closed-form solution when the effects of aerodynamic drag were considered. Solutions to the differential equations for the other cases were not found by the authors.

Combining equations (1), (4), (7), and (10) and noting from table I that $\psi=x/l$ for the vertical cylinder result in

$$mU\,dU+mg\,dx+p_0A\,dx=p_iA\left(\frac{l}{x}\right)^n dx + \frac{mg}{U_i^2}U^2\,dx \quad (17)$$

which can be written

$$\frac{dU}{dx}-\frac{g}{U_i^2}U=\left[p_iA\left(\frac{l}{x}\right)^n-p_0A-mg\right]\frac{U^{-1}}{m} \quad (18)$$

By letting

$$h=\frac{2gl}{U_i^2}$$

the solution to equation (18) is

$$U^2=e^{h\frac{x}{l}}\left\{\int e^{-h\frac{x}{l}}\frac{2}{m}\left[p_iA\left(\frac{l}{x}\right)^n-p_0A-mg\right]dx+C_2\right\} \quad (19)$$

Expressing $e^{-h\frac{x}{l}}/x^n$ in a series yields

$$\frac{e^{-h\frac{x}{l}}}{x^n}=x^{-n}-\frac{h}{l}x^{1-n}+\left(\frac{h}{l}\right)^2\frac{x^{2-n}}{2}-\left(\frac{h}{l}\right)^3\frac{x^{3-n}}{6} + \cdots\left(-\frac{h}{l}\right)^{j-1}\frac{x^{j-n-1}}{(j-1)!} \quad (20)$$

Combining equations (19) and (20), integrating, and substituting the limits $U=U_i$ for $x=l$ result in

$$\left(\frac{U}{U_i}\right)^2=e^{-h\left(1-\frac{x}{l}\right)}-\left(\frac{1}{\beta}+1\right)\left[e^{-h\left(1-\frac{x}{l}\right)}-1\right] -2e^{h\frac{x}{l}}\frac{p_iv_i}{mU_i^2}\left\{\frac{1}{1-n}\left[1-\left(\frac{x}{l}\right)^{1-n}\right]-\frac{h}{2-n}\left[1-\left(\frac{x}{l}\right)^{2-n}\right] + \cdots\frac{(-h)^{j-1}}{(j-1)!(j-n)}\left[1-\left(\frac{x}{l}\right)^{j-n}\right]\right\} \quad (21)$$

which relates the velocity of the decelerating body with the distance x and the initial conditions. The deceleration for a body with parachute drag included was previously derived and is expressed in equation (12).

For the special case where $n=0$ (constant pressure inside bag), equation (21) can be simplified considerably. The quantity within the braces reduces to

$$\frac{1}{h}\left(e^{-h\frac{x}{l}}-e^{-h}\right)$$

Then, for $n=0$, equation (21) becomes

$$\left(\frac{U}{U_i}\right)^2=1+\frac{1}{\beta}\left(\frac{p_i}{p_0}-1\right)\left[e^{-h\left(1-\frac{x}{l}\right)}-1\right] \quad (22)$$

For the special case $n=1$, equation (21) becomes

$$\left(\frac{U}{U_i}\right)^2=e^{-h\left(1-\frac{x}{l}\right)}-\left(\frac{1}{\beta}+1\right)\left[e^{-h\left(1-\frac{x}{l}\right)}-1\right] -2e^{h\frac{x}{l}}\frac{p_iv_i}{mU_i^2}\left\{\ln\frac{l}{x}-h\left(1-\frac{x}{l}\right) + \cdots\frac{(-h)^{j-1}}{(j-1)!(j-1)}\left[1-\left(\frac{x}{l}\right)^{j-1}\right]\right\} \quad (21a)$$

CALCULATION PROCEDURE

CLOSED-FORM SOLUTIONS

For the cases where there is no gas bleed from the bag ($n=\gamma$) or where the flow rate from the bag is at a rate so that the pressure within the bag is maintained at a constant value ($n=0$), closed-form dimensionless solutions are obtainable so that the velocity and deceleration can be calculated directly at any portion of the stroke. The proper equations to use for calculating deceleration characteristics are summarized as follows by equation number without suffix. Suffixes to the same basic equation number refer to special cases as discussed in the ANALYSIS section. The suffix "L" is for lunar calculations and these equations are listed in appendix B, as previously noted.

Velocity.— Equation

Case where aerodynamic drag is neglected for fully inflated bag ..... (8)

Case where aerodynamic drag is neglected for partially inflated or partially compressed bag ..... (9)

Approximate correction for aerodynamic drag ..... (16)

Case where aerodynamic drag is included for the vertical cylinder only ..... (21)

Special case where aerodynamic drag is included for vertical cylinder and bag pressure is constant ($n=0$) ..... (22)

It is not convenient to solve the equations directly to determine the value of $x/\mathscr{D}$ at which the velocity will be zero except where $n=0$ for the vertical cylinder. For the other cases, it is necessary to determine values of the velocity for a range of values of $x/\mathscr{D}$ and determine the value when the velocity is equal to zero by trial and error or by a plot of the results obtained.

Equations (8) and (9) are general equations for the following types of bags:

(1) Vertical cylinder (fig. 2(a))
(2) Horizontal cylinder (fig. 2(b))
(3) Sphere (fig. 2(c))
(4) Hemisphere (fig. 2(d))

The dimensionless terms in the velocity equations, β, $x/\mathscr{D}$, and ψ, are functions of the bag shape and are defined in table I.

Deceleration. For vehicles descending by parachute the dimensionless deceleration is calculated for the case where the bag is initially fully inflated by means of equation (12). If the bag is only partially inflated initially or is partly compressed, equation (12a) is used. The value of the velocity term in equation (12) or (12a) is obtained for the corresponding value of stroke using the appropriate equation discussed in the preceding section. If there is no aerodynamic drag, this velocity term is omitted from equations (12) and (12a). In calculating maximum decelerations, which usually occur at relatively low velocity ratios, little error results from neglecting the effect of aerodynamic drag.

To calculate the deceleration onset rate, equation (14) is used for a fully inflated bag and equation (14a) for a partially inflated bag.

The terms $\mathscr{D}$, ϵ, ψ, ψ^*, and μ used in equations (12) and (14) are functions of the bag shape and are defined in table I.

GENERAL CASE WITH GAS BLEED

By an iterative step-by-step procedure it is possible to determine the velocity and deceleration at any value of stroke for all the bag shapes considered with any schedule of gas bleed desired. Since gas will generally be bled through an orifice, the calculation method is set up to calculate bleed as a function of flow nozzle diameter. A flow nozzle type of orifice was chosen for the calculations because Reynolds number corrections can usually be neglected for this type of orifice. The procedure used is described in appendix D.

RESULTS AND DISCUSSION

The discussion of factors affecting the deceleration characteristics of gas-filled bags is complicated by the many degrees of freedom that are possible in the design. In addition to the factors affecting the thermodynamics of the deceleration, there are many practical factors as mentioned briefly in the DISCUSSION OF PROBLEM section that must be interrelated with the thermodynamic problem before an intelligent design can be made. In an effort to show the importance of some of the possible variables, a simplified analysis is first made which permits drawing some rather general conclusions on the use of gas bags for decelerating a mass during a landing impact. The effects of refinements to the analysis will be discussed subsequently. For the designer of a gas-bag impact absorption device, considerable thought will be required concerning the relative advantages and disadvantages resulting from his choice of bag shape, height, initial volume, and initial pressure before he can be sure he has arrived at a nearly optimum design. This discussion may help to channel these thoughts.

APPROXIMATE DECELERATION CHARACTERISTICS WITH NO GAS BLEED

The kinetic energy of descent can be dissipated by compression of a gas within an enclosure such as a bag. In general, however, after the decelerating vehicle has been brought to rest momentarily, the compressed gas will begin expanding and accelerate the vehicle to an upward velocity. For a descending vehicle this would result in bounce. The results to be presented for the case of deceleration without gas bleed do not consider the effects of this bounce. A method of overcoming this bounce is to deflate the bag rapidly at the instant that the velocity becomes zero. Although detailed consideration of how this deflation might be accomplished was not considered as a part of this analytical study, two general methods seem obvious. The deflation could be accomplished by rupturing, which might be actuated by internal pressure, or by mechanical means at a certain point in the deceleration stroke.

Maximum pressure and final volume. The term involving β and $x/\mathscr{D}$ in equation (8) accounts for the potential energy of the body above the ground and is of small magnitude relative to the

other terms in the equation. By neglecting this term and combining equations (7) and (8), for no gas leakage ($n=\gamma$) an equation can be written for the case where the body has been brought to rest ($U=0$) in terms of the final pressure in the bag p_f:

$$\frac{U_i^2 m}{p_i v_i}=\frac{2}{\gamma-1}\left[\left(\frac{p_f}{p_i}\right)^{\frac{\gamma-1}{\gamma}}-1\right]-2\frac{p_0}{p_i}\left[1-\left(\frac{p_i}{p_f}\right)^{\frac{1}{\gamma}}\right] \quad (8b)$$

This equation can also be written in the form

$$\frac{U_i^2 m}{p_i v_i}=\frac{2}{\gamma-1}\left[\left(\frac{v_i}{v_f}\right)^{\gamma-1}-1\right]-2\frac{p_0}{p_i}\left(1-\frac{v_f}{v_i}\right) \quad (8c)$$

These equations are represented by the solid lines in figure 3(a). The left-hand ordinate corresponds

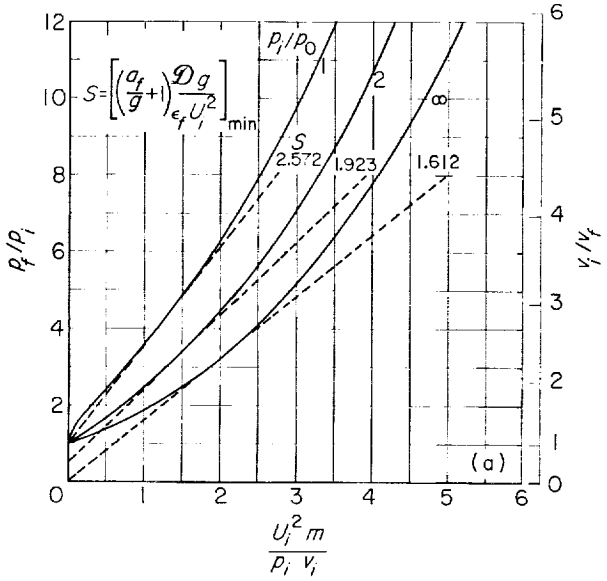

(a) Plot for determining minimum deceleration.

FIGURE 3.—Approximate relations for bringing a descending vehicle to rest on a gas-filled bag with no bleed. $\gamma=1.4$.

to equation (8b) and the right-hand ordinate is for equation (8c). The equations and the figure are for the general case and are independent of the bag shape. The curve for $p_i/p_0=\infty$ is for landing where there is no atmosphere, such as on the moon. It can be seen that for a given set of initial conditions, that is, descent velocity U_i, bag pressure p_i, atmospheric pressure p_0, and mass-to-volume ratio m/v_i, the final pressure and volume within the bag are independent of bag shape.

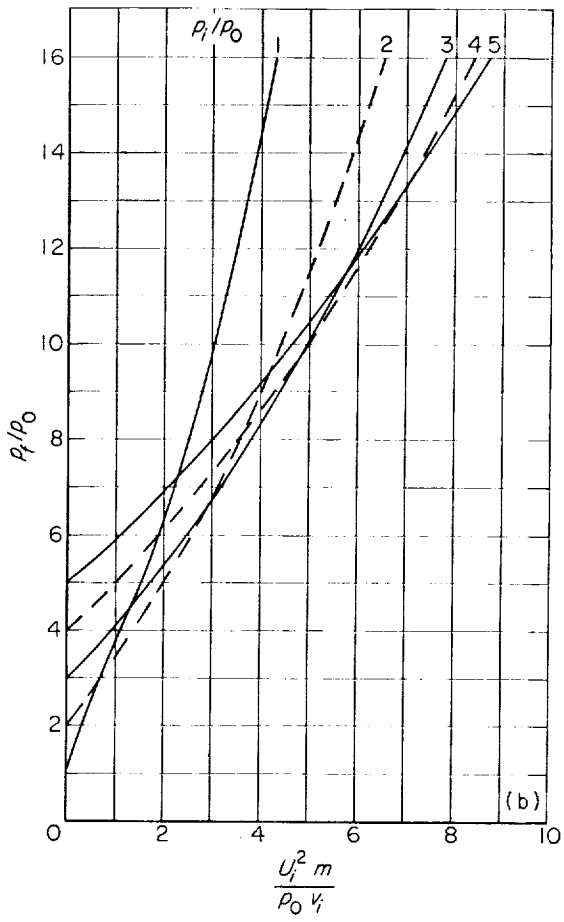

(b) Plot for determining minimum final pressure.

FIGURE 3.—Concluded. Approximate relations for bringing a descending vehicle to rest on a gas-filled bag with no bleed. $\gamma=1.4$.

Effect of initial pressure.—Equation (8b) can be readily transformed into the following form:

$$\frac{U_i^2 m}{p_0 v_i}=\frac{2}{\gamma-1}\frac{p_i}{p_0}\left[\left(\frac{p_f}{p_0}\frac{p_0}{p_i}\right)^{\frac{\gamma-1}{\gamma}}-1\right]-2\left[1-\left(\frac{p_0}{p_f}\frac{p_i}{p_0}\right)^{\frac{1}{\gamma}}\right] \quad (8d)$$

This equation is plotted in figure 3(b). It can be seen that the value of initial pressure which results in the minimum value of final pressure increases as the abscissa increases. An optimum value of initial pressure for minimizing final pressure can be found for each combination of initial velocity, mass-to-volume ratio, and atmospheric pressure.

In order to find the initial pressure that results in minimum deceleration, use can be made of equations (7) and (12) combined to yield

$$\frac{p_f}{p_i}=\frac{U_i^2}{p_i r_i}m\left[\left(\frac{a_f}{g}+1\right)\frac{\mathscr{D}g}{\epsilon_f U_i^2}\right]+\frac{p_0}{p_i} \qquad (12b)$$

This equation is plotted in figure 3(a) as shown by the dashed lines. These lines are drawn tangent to the solid curves representing equation (8b). The tangent lines represent the minimum slopes attainable for which conditions in equations (8b) and (12b) can be simultaneously satisfied. The slopes S of the dashed lines are the deceleration parameter $\left(\frac{a_f}{g}+1\right)\frac{\mathscr{D}g}{\epsilon_f U_i^2}$ and are therefore the minimum values possible for a bag with no bleed for a given initial pressure ratio p_i/p_0. A similar plot could have been made on figure 3(b), and for the same initial pressure ratio p_i/p_0 the slopes of the tangent curves would have been identical, but the added curves would have added confusion to the plot. The minimum deceleration for a given initial pressure ratio p_i/p_0 and bag height $\mathscr{D}$ occurs at the tangent point. The deceleration can be further decreased by going to higher values of initial pressure and decreasing the initial volume r_i to obtain the proper value of the abscissa (corresponding to point of tangency) in figure 3(a). If a vertical cylinder is considered which has the greatest freedom in adjusting volume and bag height independently, note that if initial height $\mathscr{D}$ is maintained the bag diameter should be decreased with increasing p_i/p_0. This results in a stability problem as previously discussed.

Increasing initial pressure to decrease deceleration soon reaches a point of diminishing return. Increasing the initial pressure ratio p_i/p_0 from 1 to 2 decreases the deceleration parameter $\left(\frac{a_f}{g}+1\right)\frac{\mathscr{D}g}{\epsilon_f U_i^2}$ by 25 percent, but going to a value of ∞ only decreases it another 12 percent relative to the value at $p_i/p_0=1$. In addition the final pressure required for obtaining minimum deceleration increases as initial pressure ratio p_i/p_0 increases so that bag strength may become a problem with high initial pressurization.

It can be concluded that the choice of initial pressure will be dependent upon the initial velocity, mass-to-volume ratio, and atmospheric pressure as well as other factors such as deceleration onset rate, bag stability, bag strength, and complications resulting from higher pressurization. Initial pressure ratios p_i/p_0 between 1 and 2 are probably within the range of most interest for landings where there is an atmosphere, as no large advantages can be found by going to higher pressures.

Effect of initial bag height.—From the parameter plotted in figure 3(a):

$$\mathscr{D}\left(\frac{a_f}{g}+1\right)=\frac{\epsilon_f U_i^2}{g}S \qquad (23)$$

From this equation the following conclusions are drawn:

(1) For all other conditions remaining constant, the final deceleration is approximately inversely proportional to the initial bag height assuming a_f/g is much larger than 1.0. The final deceleration may be different for different bag shapes, however, because of the dependency of ϵ on bag shapes as shown in table I.

(2) The minimum bag height that is possible for given initial velocity, initial pressure, and maximum permissible deceleration can be obtained from this equation. The value of mass-to-volume ratio to obtain this minimum must be chosen to give an abscissa value on figure 3(a) corresponding to the point of tangency between the solid and dashed curves.

(3) From a previous discussion it was noted that increasing the initial pressure will permit lower values of S and correspondingly lower values of $\mathscr{D}\left(\frac{a_f}{g}+1\right)$. This increased pressure could be utilized to decrease either deceleration or initial bag height. It should be noted that, for the case where there is no atmosphere ($p_i/p_0=\infty$), the deceleration or bag height can be cut about 37 percent from the value required where there is an atmosphere and the initial bag pressure is equal to the atmospheric pressure.

Effect of bag shape.—The kinetic energy of the descending vehicle must be absorbed by the work in compressing the gas in the bag. The net work is $\int_{\mathscr{D}}^{x_f} A(p-p_0)\mathrm{d}x$, and it is the same for all bag shapes. As discussed previously for the same initial conditions (p_i, p_0, m/r_i, $\mathscr{D}$, and U_i), the final pressure is also the same for all bag shapes. The contact area A does not vary with stroke for

the vertical cylinder, but for the other bag shapes the area increases with stroke. The final area A_f for these shapes must be higher than that of the vertical cylinder with the same stroke in order for the mean area to be approximately the same for all cases. The effect of this final area on deceleration can be seen from equation (12b), which can be written in the form

$$\frac{a_f}{g}=\frac{A_f}{gm}(p_f-p_0)-1 \tag{12c}$$

With the same final pressure p_f for all shapes, this equation suggests that the maximum deceleration required to bring a body to rest is lower for the vertical cylinder than for the other shapes.

Effect of mass-to-volume ratio. —The point of tangency of the curves in figure 3(a) represents the conditions that result in minimum deceleration or required bag height. For specified values of initial pressure and initial velocity, it can therefore be seen that there is an optimum value of mass-to-volume ratio m/v_i that results in an abscissa value corresponding to the tangency point. Going to higher or lower values can result in increased decelerations or higher required initial bag heights. This is not a marked effect, however, since the curves are approximately tangent for a fairly large distance. From the figure it can be seen that for $1\leq p_i/p_0\leq 2$ the mass-to-volume ratio represented by

$$\frac{m}{v_i}\approx 1.35\frac{p_i}{V_i^2} \tag{24}$$

results in minimum deceleration or bag height. This value of mass-to-volume ratio also specifies the compression ratio in the bag for a given value of p_i/p_0. To reduce the final pressure the initial volume could be increased, which would result in a smaller mass-to-volume ratio than the optimum, but it would reduce required bag strength with a very small penalty in maximum deceleration developed. The significance of variations in m/v_i will be further discussed subsequently.

REFINED DECELERATION CALCULATIONS WITH NO GAS BLEED

The conclusions based on the approximate calculations just discussed are generally valid for gas bags without bleed. In the remainder of the report, a more exact evaluation will be made of effects such as parachute drag, bag shape, and gas bleed. In addition values of deceleration, pressure, velocity variation, and deceleration onset rate that can be expected for specific conditions will be presented in the figures and table II. Calculations were made for four bag shapes, namely, the vertical cylinder, horizontal cylinder, sphere, and hemisphere. The results are presented for landing on earth at sea level at velocities from 20 to 40 feet per second, which is consistent for descent by parachute. The value of n used in the calculations was 1.40, which makes the results valid for many gases of interest such as air, nitrogen, hydrogen, and oxygen. For deceleration on a moon or planet different from the earth, the gravitational constant in the β term would be different from the value of 32.17 feet per second squared used herein. The effect of atmospheric pressure is also included in the β term.

In this analysis the assumption is made that the compression of the gas is isentropic and the temperature and pressure are uniform throughout the bag volume. Such an assumption limits the validity of the analysis to impact velocities which are low compared to the sonic velocity of the gas within the bag. At high impact velocities a wave analysis similar to that of reference 10 for high-velocity impact of spheres is required. At these high velocities the compression remains essentially adiabatic, but it is not isentropic. As a result, for a given amount of energy imparted to the gas from the kinetic energy of the descending vehicle the pressure rise in the gas will be less than for an isentropic compression. Since the deceleration is a function of the pressure within the bag, the maximum deceleration calculated by this isentropic compression analysis will be higher than would be actually encountered with a high-speed impact. In addition the calculated stroke required to stop the vehicle would be lower than actually encountered. This error is probably negligible, particularly for the vertical cylinder, for most impact speeds of interest. Calculations for the vertical cylinder have indicated that the pressure calculated by a wave analysis is very nearly the same as for isentropic compression for impact velocities up to at least 20 percent of the sonic velocity within the gas. The error is much greater, however, for the other configurations. The analysis is applicable for higher impact velocities for light gases such as hydrogen than for heavier gases because of the higher sonic velocity of the light gases. A further

advantage of a light gas for lunar landings would be the reduced weight required for transporting it. As stated previously, the equations in appendix B should be used for calculations for lunar landings.

Effect of parachute drag.—When a body is descending at a constant velocity, parachute drag is equal to the weight of the descending body. At this condition the force of the body is 1.0 g. As the descent velocity is slowed by a gas bag, the parachute drag force diminishes rapidly since drag forces usually vary as the square of the velocity. As a result, it would be expected that the effects of parachute drag would be relatively small on deceleration characteristics. This effect is illustrated in figure 4, where results from equations (8) and (21) are compared to show the effect of neglecting parachute drag in the velocity equation for a vertical cylinder. Parachute drag is considered in the deceleration equation, but the deceleration calculated is affected slightly by the velocity term (see eq. (12)). Therefore, neglecting parachute drag in the velocity equation results in a very small effect in the calculated deceleration. Figure 4 shows that by neglecting parachute drag in the velocity equation the calculated stroke is slightly high. As a result, the maximum deceleration which occurs when zero velocity is attained is calculated for too high a stroke and therefore is also somewhat high.

Calculations were also made to determine the velocity as a function of stroke with the effects of parachute drag included by use of the approximate velocity equation (16). For the case where the increment of stroke Δx was 0.05 l, the results were almost identical to the results from the exact equation (21). When a value of Δx equal to 0.10 l was used in the approximate solution, however, the calculated velocities were too low. It appears, therefore, that equation (16) can be used, and it will give relatively accurate results if small increments of stroke are used in the calculations. Actually, the true deceleration characteristics probably lie somewhere between those calculated including parachute drag and those neglecting drag. During the deceleration process in which the vehicle and parachute are rapidly slowing down, some of the air under the parachute tends to be moving downward faster than the parachute because of momentum it has developed while being trapped under the parachute. This effect would result in the parachute drag not being proportional to the square of the sinking velocity; consequently, the parachute drag would be less than calculated herein.

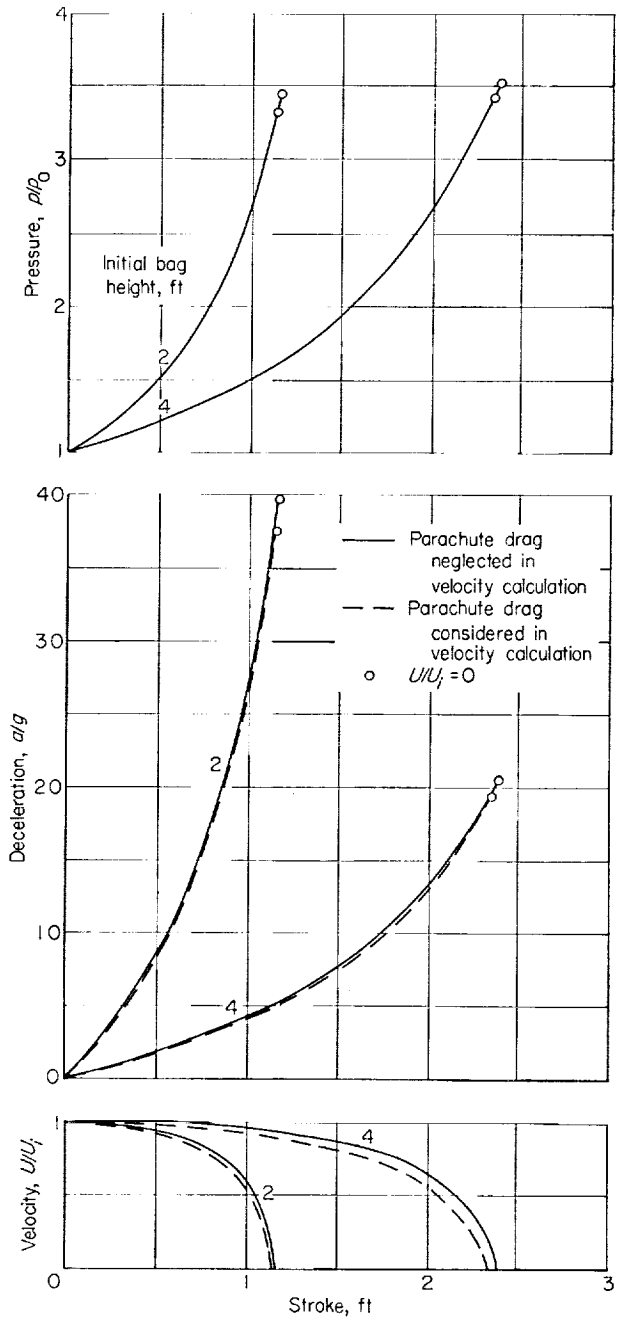

FIGURE 4.—Effect of neglecting parachute drag for vertical cylinder velocity calculations. $U_i=30$ feet per second; $p_i/p_0=1.0$; $m/v_i=2$ slugs per cubic foot; no bleed.

It appears that calculations neglecting parachute drag are slightly conservative, and appreciable

errors are not encountered. As a result, parachute drag was neglected in most of the velocity calculations. This permitted use of closed-form solutions for all bag shapes studied.

Effect of initial bag pressure.—For practical purposes it is desirable to inflate the bag to as low a gage pressure as possible. If the internal absolute pressure of the bag could be the same as the external pressure, a pressurization bottle or pump could possibly be avoided. In this manner the bag could be opened by gravity or some type of spring action and filled to atmospheric pressure through a one-way valve by natural aspiration. The effect of initial bag pressure on deceleration characteristics is shown in figure 5, where the

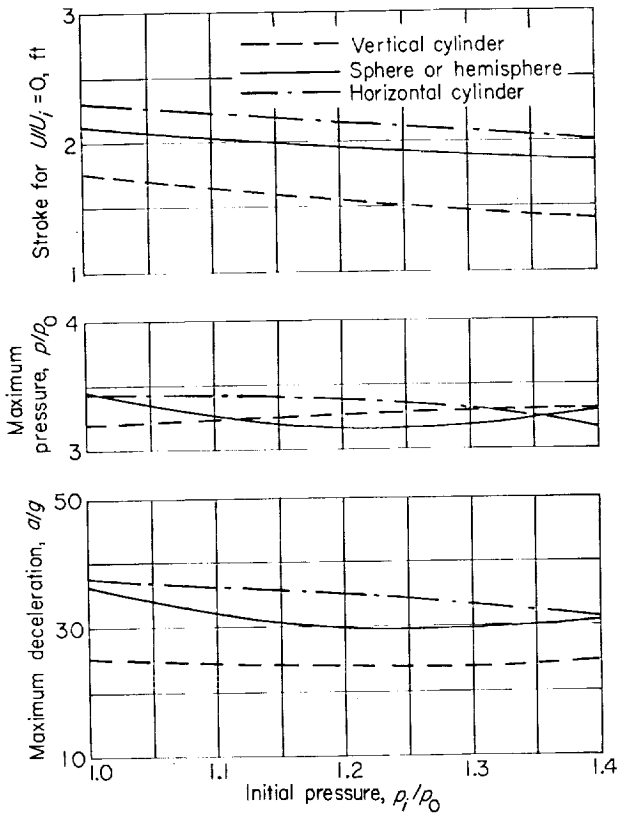

FIGURE 5.—Effect of initial bag pressure on deceleration characteristics. U_i=30 feet per second; $\mathscr{D}$=3 feet; m/v_i=2 slugs per cubic foot; no bleed.

ratio of initial pressure to atmospheric pressure is plotted against the maximum deceleration, pressure, and stroke required to decelerate to zero velocity. The comparison is made for the four bag shapes considered in this analytical study.

The value of $U_i^{-2}m/p_0v_i$ (see fig. 3(b)) used for these calculations is in the range (0.85) where it would be expected that the initial pressure range considered in figure 5 would have little effect on the final pressure. For the vertical cylinder it would follow that deceleration would not be appreciably affected either. This is verified in figure 5. The approximate analysis also indicated that the final deceleration would be affected by bag shape. Figure 5 shows that the effect of bag shape on deceleration can amount to as much as 50 percent. In addition, the deceleration variation due to initial pressure ratio variation from 1.0 to 1.4 can amount to about 20 percent for shapes other than the vertical cylinder. As previously discussed, this deceleration could be decreased by an increase in bag height.

Table II shows values of the maximum deceleration onset rates $\dot{a}/g$ encountered during the deceleration process for all cases considered in this analysis. The figure number is listed that presents other deceleration characteristics for the same conditions. The values listed for the vertical cylinder for initial pressure ratios of 1.2 and 1.4 are values after initial impact. At the moment of impact the onset rate is theoretically infinity. This is an undesirable characteristic that occurs only with the vertical cylinder for a perfectly alined impact on the flat end of the cylinder. This effect and the allowable values of onset rates will be discussed in more detail later.

Since most of the conditions considered in illustrating the effects of various factors on deceleration characteristics are in the range where initial pressure will not have a significant effect, most of the results in the remainder of the report will be for the initial pressure equal to atmospheric pressure.

Effects of initial velocity, bag height, and mass-to-volume ratio.—Figure 6 shows how the maximum deceleration, maximum pressure, and stroke are affected by the initial velocity and mass-to-initial-bag-volume ratio for initial bag heights of 2, 3, and 4 feet. The comparisons are made for an atmospheric initial bag pressure. In general the behavior is the same as predicted by the approximate calculations. Maximum deceleration is approximately inversely proportional to initial bag height. Maximum bag pressure and maximum deceleration both increase approximately as the square of the initial velocity.

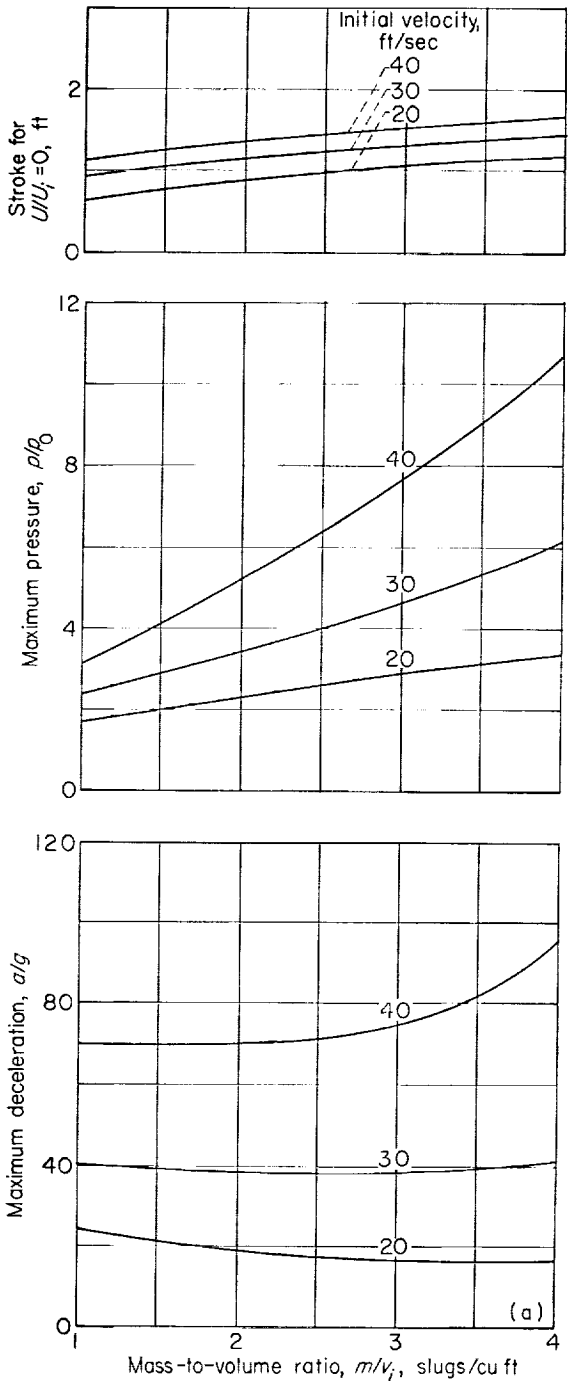

(a) Initial bag height, 2 feet.

FIGURE 6.—Maximum deceleration, pressure, and stroke for vertical cylinder. $p_i/p_0=1.0$; no bleed.

Equation (24) indicates that the values of m/v_i that would result in minimum deceleration would be about 7.1, 3.2, and 1.8 slugs per cubic foot for initial velocities of 20, 30, and 40 feet per second, respectively. The m/v_i range for 20 feet per second was not carried this far, but it is indicated in figure 6 that these values are approximately correct for the three bag heights considered. It should also be noted, however, that substantial variation in mass-to-volume ratio is

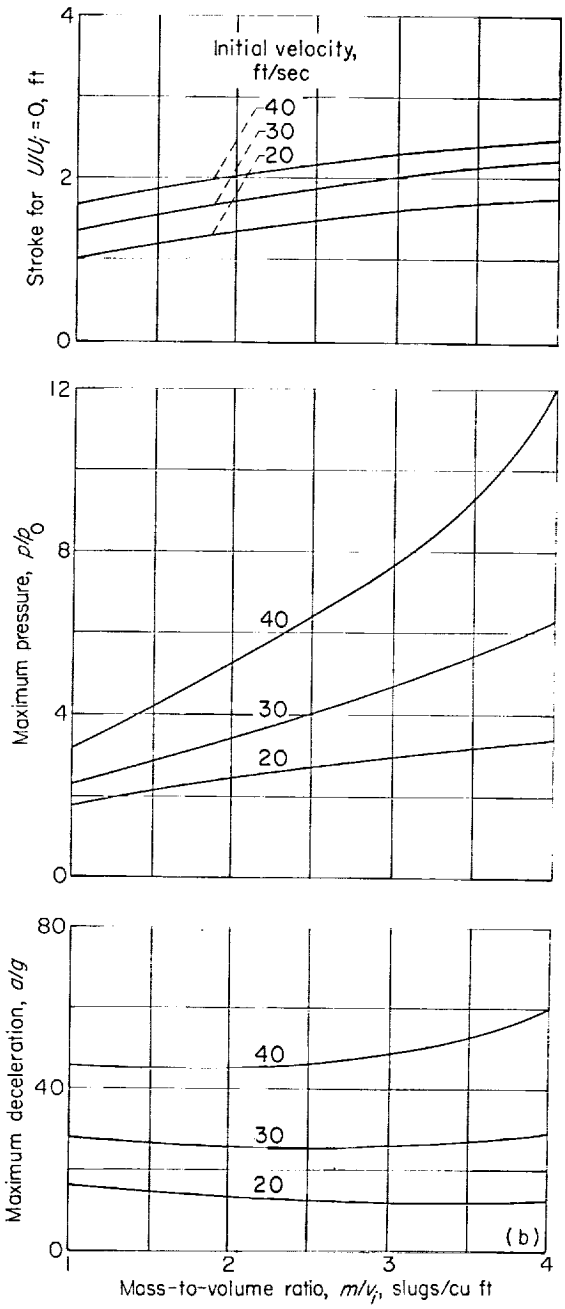

(b) Initial bag height, 3 feet.

FIGURE 6.—Continued. Maximum deceleration, pressure, and stroke for vertical cylinder. $p_i/p_0=1.0$; no bleed.

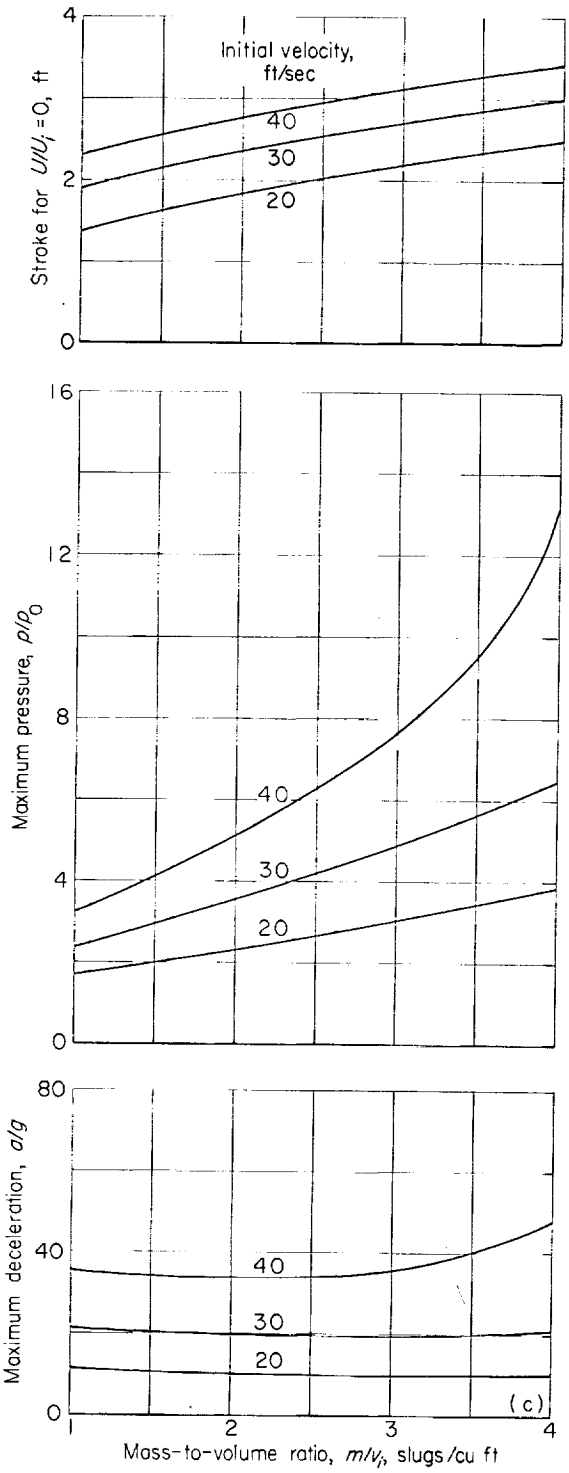

(c) Initial bag height, 4 feet.

FIGURE 6.—Concluded. Maximum deceleration, pressure, and stroke for vertical cylinder. $p_i/p_0=1.0$; no bleed.

permissible with only slight effects on deceleration. This is very fortunate. For a vehicle with a number of individual bags around its periphery, a cocked descent, so that only a portion of the bags impact, will not result in excessive decelerations. If the bags are designed to withstand the higher pressures that result for the higher mass-to-volume ratios for those particular bags, the deceleration can be accomplished satisfactorily.

Figure 6 indicates that for the range of initial velocities considered a mass-to-volume ratio of about 2 slugs per cubic foot is reasonable. This corresponds to about 1 cubic foot of gas-bag volume for every 65 pounds of vehicle weight.

Table II lists the maximum deceleration onset rates $\dot{a}/g$ encountered during the deceleration process. In reference 11 data are shown where a human has been subjected to an onset rate of 1156 g's per second with a maximum deceleration of 35 g's without debilitating results. It is indicated from results of chimpanzee exposures that humans may be able to tolerate higher onset rates, but the debilitating effects of shock may result. Chimpanzees have survived maximum exposures of 34.2 g's at 3350 g's per second. Although otherwise uninjured, they sustained cardiovascular shock. Reference 11 also indicates that about 35 g's is the maximum safe deceleration for exposures up to 0.1 second. Table II indicates onset rates exceeding a value of 1200 g's per second by footnote reference mark c. From the results presented in figure 6 and table II it can be seen that the safe onset rate is only exceeded for the cases where the maximum safe deceleration is also exceeded.

Bag shape.—The effect of bag shape on deceleration characteristics is shown in figure 7. It can be noted that the vehicle can be brought to rest in a shorter distance at a lower maximum deceleration with a vertical cylinder than with the other shapes. This effect was noted and discussed in connection with figures 3 and 5. A considerable portion of the stroke is used up before contact area, and internal volume changes enough for the sphere, hemisphere, and horizontal cylinder to significantly affect pressure and deceleration. About 50 percent of the available stroke is used up with these bag shapes before the vehicle starts slowing down an appreciable amount.

Although the results of this analysis were only for vertical descent, some consideration should be given to side drift and cocked impact. As pre-

viously discussed, cocked impact on multiple bags of a vertical cylinder type would probably be all

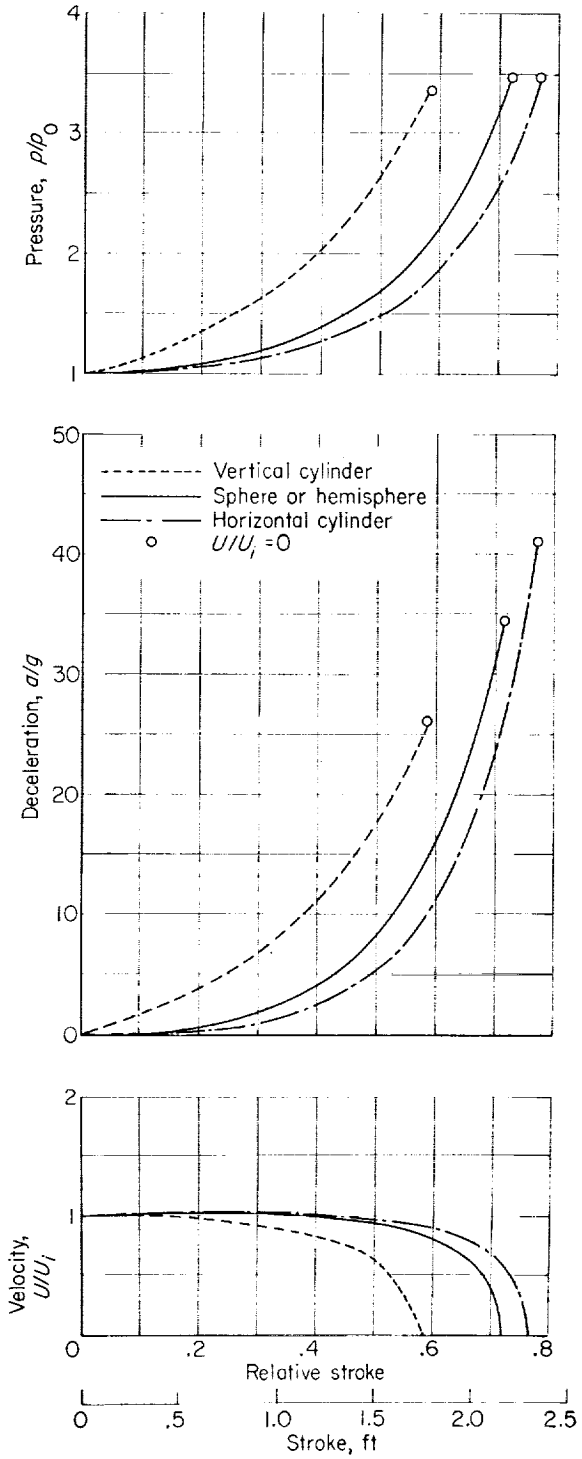

FIGURE 7.—Effect of bag shape on impact characteristics. U_i=30 feet per second; $\mathscr{D}$=3 feet; m/v_i=2 slugs per cubic foot; p_i/p_0=1.0; no bleed.

right so long as the bags in contact with the ground could withstand the added internal pressure, but with side drift vertical bags would tend to bend, collapse, or tear loose. The hemispherical bag should have less tendency than any of the other shapes to fail in such a manner in a landing with side drift. A big disadvantage of bag shapes other than the vertical cylinder, however, is that there is less freedom in the choice of variations between bag height and initial volume. From an overall point of view, a multiple-bag arrangement of vertical cylinders probably has the most potential of the shapes studied.

DECELERATION WITH GAS BLEED

For the cases considered thus far where no gas was bled from the bag during the deceleration of the body, the pressures within the bag and the decelerations can build up to values that may be too high to be acceptable. In addition, the pressure energy that builds up in the bag will cause the vehicle to bounce upwards after dissipation of the sinking speed. A logical method of overcoming these difficulties is to provide a method of bleeding gas from the bag. Three general bleed methods were considered: (1) the rather idealized case for bleed to maintain constant pressure within the bag, (2) instantaneous partial bleed by letting part of a multiple-bag system burst, and (3) bleed from a fixed-area orifice.

Constant-pressure bleed.—Figure 8 compares the deceleration characteristics of the different bag shapes for the case where the pressure within the bag is maintained constant. To obtain this condition would require an initial pressurization device and a variable-area orifice that would be pressure-actuated. Comparing figures 7 and 8 shows that the constant-pressure bleed results in stopping the vehicle in less distance at lower maximum deceleration. The deceleration is almost constant over the entire stroke for the vertical cylinder. The only variation in deceleration is due to the variation in parachute drag as velocity decreases. For the other bag shapes the deceleration steadily increases with increasing stroke because of an increase in contact area as the bag is compressed. The effect of including parachute drag in the velocity calculations is also shown in the figure for the vertical cylinder. As was illustrated in figure 4 for no gas bleed, the accuracy of the calculation is not seriously affected

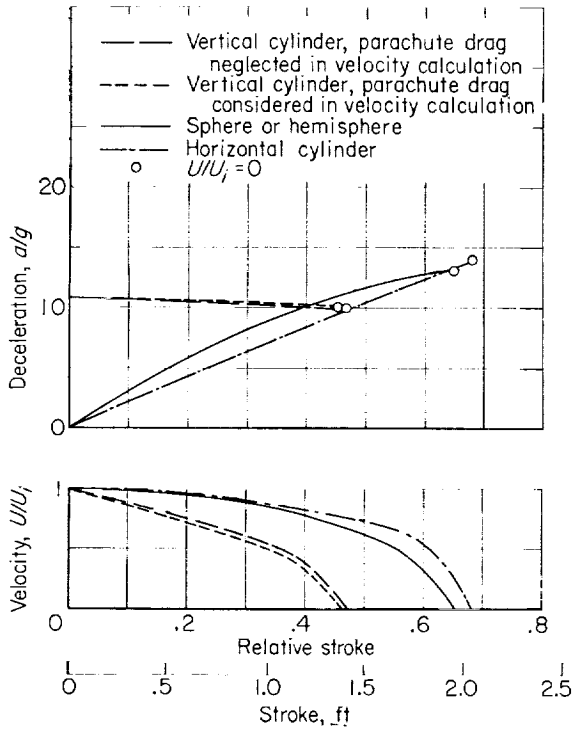

FIGURE 8. -Effect of bag shape on impact characteristics for constant-pressure bleed. $U_i = 30$ feet per second; $\mathscr{L} = 3$ feet; $m/v_i = 2$ slugs per cubic foot; $p/p_0 = 2.0$.

by neglecting parachute drag effects in the velocity equation. The effect of this drag is always included in the deceleration equations.

Table II shows that for a vertical cylinder and constant bag pressure the deceleration onset rate is theoretically infinite. This infinite rate results from the discontinuous deceleration which changes from zero to about 11 g's at the moment of impact. After impact the onset rates are slightly negative because the deceleration is decreasing with stroke. Methods of overcoming this infinite onset rate will be discussed later.

Figure 9 shows a more practical application of the constant-bleed pressure system. For this case the initial pressure in the bag is atmospheric, and the orifice is plugged to permit a pressure buildup in the bag during the initial portion of the stroke. At some pressure corresponding to a specified deceleration, 10 g's for figure 9, the plug would blow out of the variable-area orifice, and the pressure would be maintained constant for the rest of the stroke. This procedure results in onset rates (table II) that are acceptable. A greater stroke is required, however, than for the case with no bleed shown in figure 7.

In addition to the advantage of the bleed system being able to stop the vehicle at lower maximum deceleration than the no-bleed system, another very distinct advantage is the reduction of bounce after the sinking speed is brought to zero. Without a bleed system, a method of rupturing the bag would be required at the end of the stroke to reduce bounce as previously discussed. Rupturing, which could be either pressure- or distance-actuated, suffers from a disadvantage for cocked descents or impact on uneven terrain. For these cases the rupturing might not occur at the proper portion of the stroke. For this reason, it appears to be very desirable to bleed gas from the bags during the compression stroke.

Optimum bag shape.—If the optimum shape is defined as that resulting in the shortest stroke within given limitations of deceleration and deceleration onset, the optimum design would result in a linear deceleration buildup to the maximum value, and then this value of deceleration would be maintained until the body was

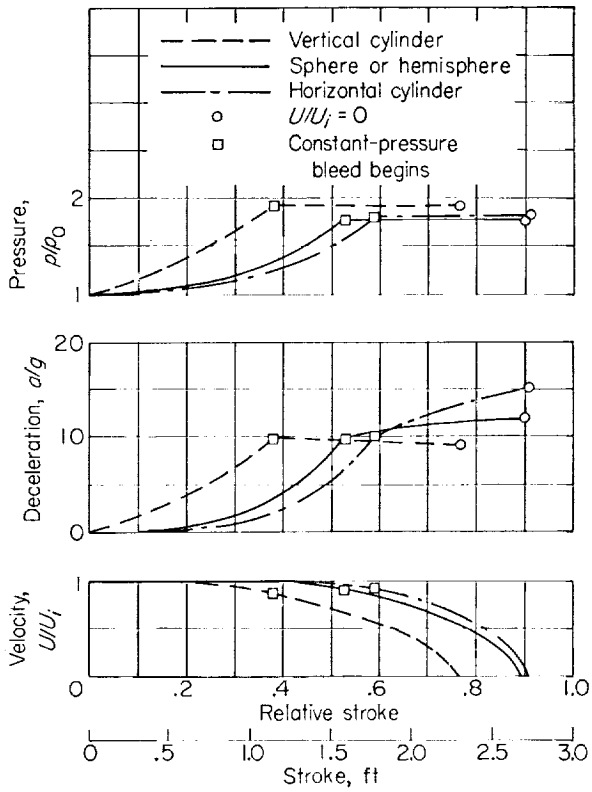

FIGURE 9. - Effect of bag shape on impact characteristics for constant-pressure bleed after reaching deceleration of 10 g's with no bleed. $U_i = 30$ feet per second; $\mathscr{L} = 3$ feet; $m/v_i = 2$ slugs per cubic foot; $p_i/p_0 = 1.0$.

brought to rest. Figures 8 and 9 show that using a vertical cylinder and a bleed rate that maintains constant pressure results in essentially constant deceleration. The variation from constant deceleration results from parachute drag variations due to change in velocity. If a paraboloid of height $U_i\frac{(a/g)_{max}}{(\dot{a}/g)_{max}}$ feet is attached to the bottom of the vertical cylinder and constant internal bag pressure is maintained at a value that will result in $(a/g)_{max}$ for the vertical cylinder, the deceleration will vary linearly with stroke up to its maximum value and will then remain at essentially this maximum value until the vehicle comes to rest. Such a configuration would very closely approximate the optimum bag shape. This configuration would require pressurization prior to impact.

Instantaneous bleed.—In an effort to determine if maximum decelerations could be decreased in some manner without increasing bag height or using gas bleed from an orifice, an analysis was made of cases where multiple bags would be used on the bottom of the vehicle and part of the bags would burst at some predetermined deceleration level. Figure 10 illustrates the case where the bags are of two different heights, with the heights and bag rupturing strength chosen so that the bags were useful for different parts of the stroke. At initial contact with the terrain, only part of the bags would be in contact with the terrain. These bags would decelerate the vehicle until the deceleration had built up to 10 g's. At this point, the second set of bags would come in contact with the terrain and the first set of bags would rupture. This would reduce the deceleration to zero momentarily, and the deceleration would start building up again. Two mass-to-volume ratios were investigated for the second portion of the stroke, and it was found that in both cases the maximum decelerations were greater than would have been encountered if only one set of bags had been utilized over the entire stroke. It can be concluded, therefore, that this deceleration method is not desirable.

A somewhat similar case was investigated in figure 11. In this case, all the bags made initial contact with the terrain, but part of them burst after the deceleration built up to a value of 10 g's. Cases were considered where half of the bags burst (doubling the value of m/r_i) and where

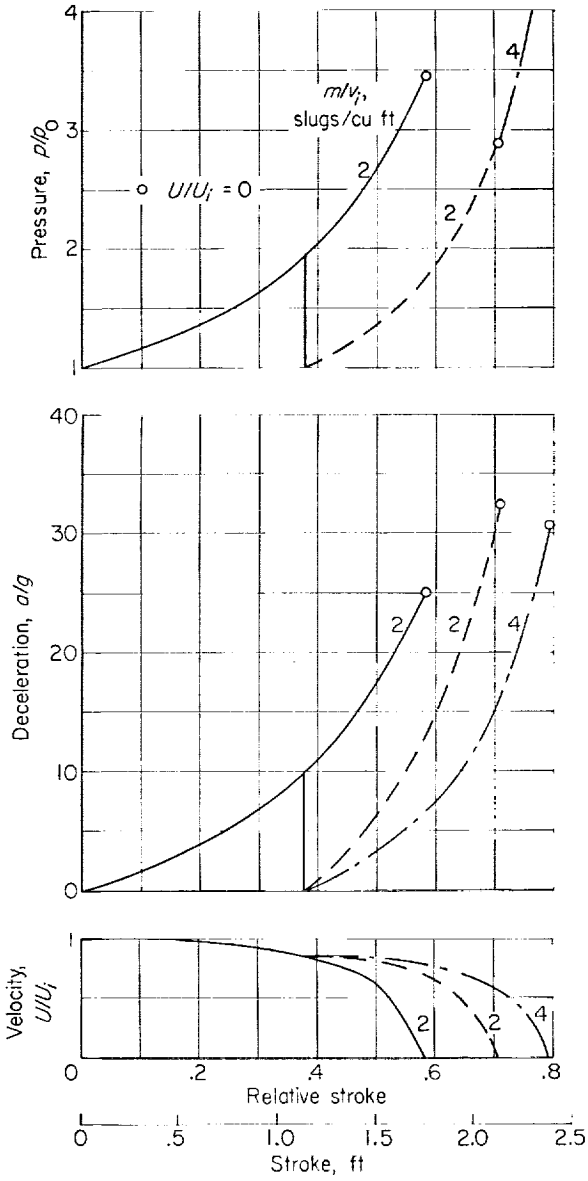

FIGURE 10. Effect of deceleration by steps with initial bag bursting at a deceleration of 10 g's. Vertical cylinder; U_i=30 feet per second; l=3 feet; p_i/p_0=1.0.

two-thirds of the bags burst (tripling the value of m/r_i). As can be seen from figure 11, this procedure does not appreciably affect the maximum deceleration, but it does substantially increase the maximum pressure. It was therefore concluded that this method of deceleration was undesirable also.

Fixed-orifice-area bleed.—Figure 12 shows the deceleration characteristics with fixed-area bleed orifices for three different orifice sizes. In figure

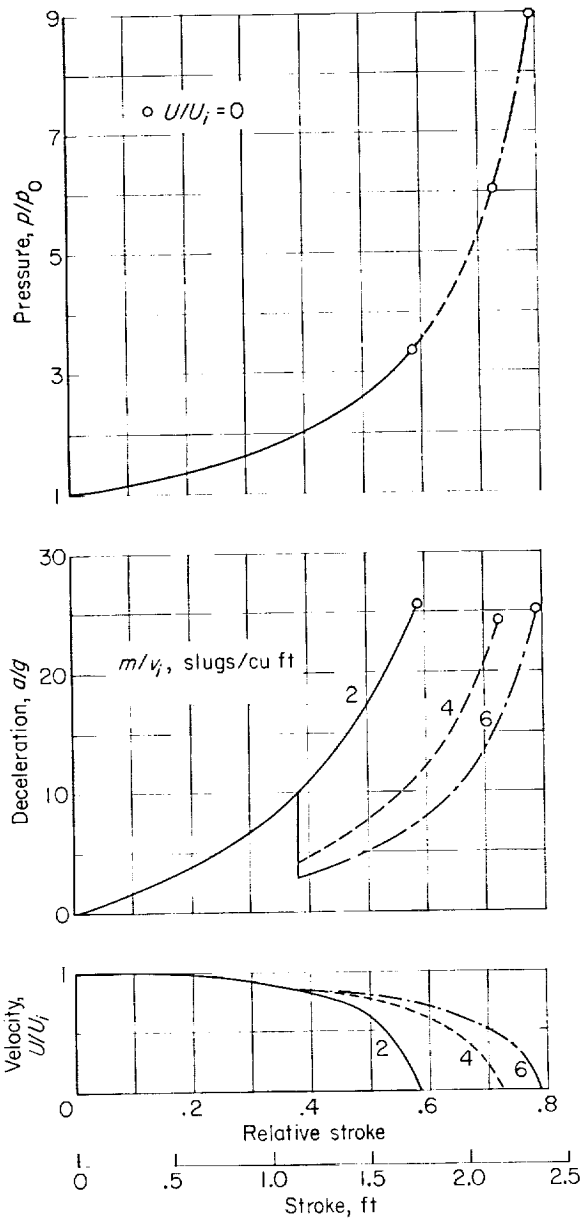

FIGURE 11. Deceleration characteristics with one-half and two-thirds of bags bursting at initial deceleration of 10 g's. Vertical cylinder; $U_i=30$ feet per second; $l=3$ feet; $p_i/p_0=1.0$.

12(a) the case was considered where the orifices were plugged until the pressure in the bag had built up to a point where the deceleration was 10 g's. At this point the orifice became unplugged, and gas was bled from the bag. The rate of gas bleed for a given orifice size is a function of the pressure within the bag. Only relative orifice sizes are given in the figure. The actual size required is a function of the initial volume of the bag and the gas used. For a relative area of 1, $KA_f=3.67\times10^{-3}v_i$ square foot for air as the gas in the bag. Other areas considered were two and four times this value.

Comparing figure 12(a) and the vertical cylinder portion of figure 7 shows that the stroke is not significantly affected, but the maximum deceleration is reduced for relative orifice sizes of 1 and 2. Going to a relative orifice size of 4, however, results in a case where the vehicle has not been brought to rest before the end of the stroke because of too much gas being bled from the bag by the large orifice. As a matter of fact, the vehicle reaches a minimum velocity and then starts accelerating again because of the gravitational effect.

In figure 12(b) the case is considered where air is bled from the orifice for the entire stroke. For this case it is only with the smallest orifice that the vehicle is brought to rest before the end of the available stroke. With the largest orifice only 20 percent of the velocity has been dissipated at the end of the stroke. Such an arrangement would result in a disastrous landing. It appears that, because of the shorter period of time when the orifice is used when it is plugged during the first portion of the stroke (fig. 12(a)), a greater variation in orifice area may be permissible than for the case where gas is bled from the orifice for the entire stroke. Another advantage to using a plugged orifice for a portion of the stroke is a shorter stopping distance with about the same maximum deceleration.

Calculations were made to check the effect of assumptions and approximations used in the stepwise solution (appendix D) on the solution's accuracy. Iterative calculations where the orifice was so small as to cause negligible bleed were made, and results were compared with the closed-form solutions with no bleed. The difference in the two solutions could not be detected when plotted on curves to the scale used in this report for a time increment $\Delta t\approx\frac{1}{20}\frac{g}{U_i}$. This time increment results in approximately 10 increments in stroke between impact and zero velocity.

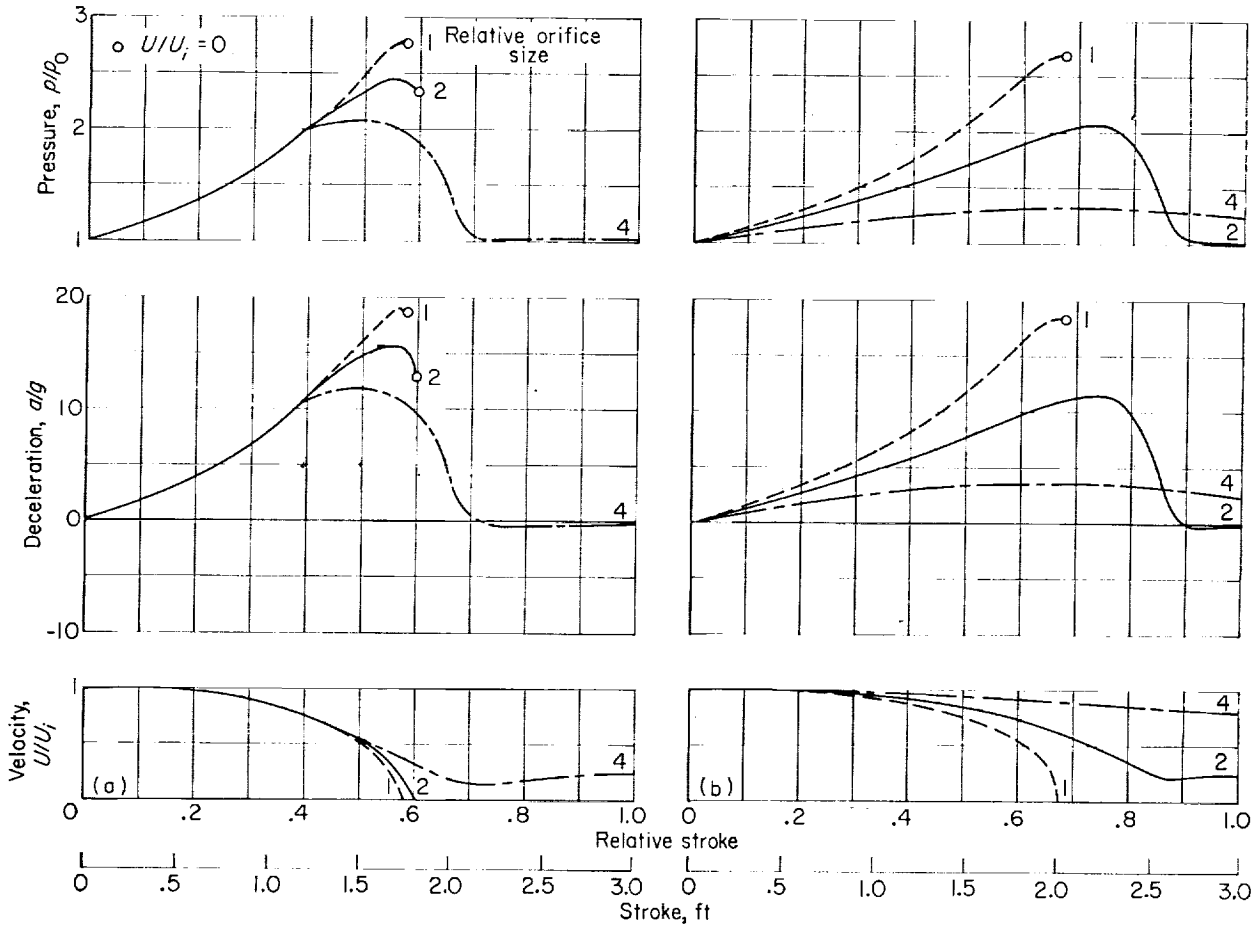

(a) No bleed until $a/g = 10$.

(b) Fixed bleed for entire stroke.

FIGURE 12.—Deceleration characteristics using fixed-area bleed orifices. Vertical cylinder; U_i=30 feet per second; l=3 feet; m/v_i=2 slugs per cubic foot; p_i/p_0=1.0.

CONCLUDING REMARKS

The following conclusions can be drawn from the results of this analytical study:

1. An analytical procedure is developed that permits calculation of velocity, deceleration, and deceleration onset rate as a function of distance traversed after impact on gas-filled bags having a variety of shapes. The analysis is applicable to planetary or lunar landings for sinking speeds that are low compared to the sonic velocity of the gas within the bag. For relatively high sinking speeds a light gas such as hydrogen or helium should probably be used.

2. Gas-filled bags can be used to absorb landing shocks for normal parachute sinking speeds with deceleration and onset rate acceptable for well-supported human beings.

3. Acceptable onset rates for humans were found to be exceeded only when the landing conditions resulted in the deceleration rates being too high, except for special cases where the bags of the vertical cylinder configuration were pressurized above atmospheric prior to impact.

4. From the standpoints of maximum deceleration and required stroke, the vertical cylinder appears to be the best shape studied. Multiple

bags should probably be used, however, to accept cocked impacts. A cocked impact where only part of the bags would be active would not appreciably increase the deceleration rates, but bag pressures would be increased.

5. For earth landings using parachutes, a reasonable bag volume is about 1 cubic foot for each 65 pounds of vehicle.

6. A method of controlled gas bleed from the bags is required. The ideal method would be to utilize pressure-actuated orifices of variable area that could maintain constant pressure. Bags with constant-area orifices of the proper size would be satisfactory, but would require a somewhat greater stroke for a given maximum deceleration. It would be possible, however, to utilize bags without bleed during the deceleration process, but the bags would have to be deflated rapidly at the end of the stroke to eliminate or reduce bounce.

LEWIS RESEARCH CENTER
NATIONAL AERONAUTICS AND SPACE ADMINISTRATION
CLEVELAND, OHIO, *March 16, 1960*

APPENDIX A

SYMBOLS

A	bag area in contact with ground, sq ft
A_D	drag area, sq ft
A_n	area of orifice or flow nozzle, sq ft
a	deceleration, ft/sec^2
b	dimension of flattened portion of bag, ft (see fig. 2)
C_D	aerodynamic drag coefficient
C_1, C_2	numerical constants
D	fully inflated bag diameter (horizontal cylinder and sphere), ft
$\mathscr{D}$	fully inflated bag height, ft, see table I
g	local gravitational acceleration, ft/sec^2
h	dimensionless term, $2gl/U_i^2$
j	number of terms in a series
K	flow nozzle coefficient
L	bag length (horizontal cylinder), ft
l	fully inflated bag height (vertical cylinder), ft
M	gas Mach number
m	mass of entire vehicle, (lb)(sec^2)/ft (or slugs)
n	exponent having a value less than or equal to γ
P	perimeter, ft
p	static pressure (without subscript refers to gas in bag), lb/sq ft abs
p^*	static pressure in bag at bag height equal to x^*, lb/sq ft abs
R	gas constant, ft/°R
r	radius of hemisphere, ft
S	slope of line, fig. 3(a)
T	temperature, °R
t	time, sec
U	velocity, ft/sec
U^*	velocity at bag height equal to x^*, ft/sec
u	gas velocity in nozzle, ft/sec
v	volume, cu ft
W	weight of gas in bag, lb
$\dot{W}$	weight rate of flow, lb/sec
x	distance, ft
x^*	partially inflated initial bag height, ft
β	dimensionless ratio, $mg\mathscr{D}/v_i p_0$, see table I
γ	ratio of specific heats of gas in bag
ϵ	dimensionless ratio, $A\mathscr{D}/v_i$, see table I
ζ	pressure function in orifice equation
λ	dimensionless density, ρ/ρ_i
μ	dimensionless ratio, $\dot{\epsilon}\frac{\mathscr{D}}{U}$, see table I
ρ	density, lb/cu ft
ψ	dimensionless volume, v/v_i, see table I
ψ^*	dimensionless volume at bag height equal to x^*
Ω	pressure function in orifice equation

Subscripts:

a	approximate value
f	final value
i	initial value
max	maximum value
min	minimum value
n	flow nozzle
t	flow nozzle throat
x	at position x
$x+\Delta x$	at position $x+\Delta x$
0	atmospheric

Superscripts:

—	average value over increment Δx
.	d/dt

APPENDIX B

EQUATIONS FOR LUNAR LANDINGS

Equations presented in this appendix have been rearranged to permit their use for the case where $p_0=0$. These equations have the same numbers as in the body of the report except they are followed by the suffix L. These equations are not to be used for $p_0\neq 0$.

$$\left(\frac{U}{U_i}\right)^2=1+\frac{2v_ip_i}{mU_i^2}\left[\frac{mg\mathscr{D}}{v_ip_i}\left(1-\frac{x}{\mathscr{D}}\right)-\frac{1}{n-1}(\psi^{1-n}-1)\right] \tag{8L}$$

$$\left(\frac{U}{U_i}\right)^2=1+\frac{2v_ip_i}{mU_i^2}\left[\frac{mg\mathscr{D}}{v_ip_i}\left(1-\frac{x}{\mathscr{D}}\right)-\ln\frac{1}{\psi}\right] \tag{8aL}$$

$$\left(\frac{U}{U^*}\right)^2=1+\frac{2v_ip^*}{mU_i^2}\left\{\frac{mgx^*}{v_ip^*}\left(1-\frac{x}{x^*}\right)+\frac{(\psi^*)^n}{n-1}[(\psi^*)^{1-n}-\psi^{1-n}]\right\} \tag{9L}$$

$$\left(\frac{U}{U_i}\right)^2=1+\frac{2v_ip^*}{mU_i^2}\left[\frac{mgx^*}{v_ip^*}\left(1-\frac{x}{x^*}\right)+\psi^*\left(\ln\frac{1}{\psi^*}-\ln\frac{1}{\psi}\right)\right] \tag{9aL}$$

$$\frac{a}{g}=\frac{v_ip_i}{mg\mathscr{D}}\epsilon\psi^{-n}+\left(\frac{U}{U_i}\right)^2-1 \tag{12L}$$

$$\frac{a}{g}=\frac{v_ip^*\epsilon}{mg\mathscr{D}}\left(\frac{\psi}{\psi^*}\right)^{-n}+\left(\frac{U}{U^*}\frac{U^*}{U_i}\right)^2-1 \tag{12aL}$$

$$\frac{\dot{a}}{g}=\frac{U}{U_i}\left[\frac{v_ip_iU_i\psi^{-n}}{mg\mathscr{D}^2}\left(\frac{n\epsilon^2}{\psi}+\mu\right)-\frac{2q}{U_i}\left(\frac{a}{g}\right)\right] \tag{14L}$$

$$\frac{\dot{a}}{g}=\frac{U}{U^*}\left[\frac{v_ip^*U^*}{mg\mathscr{D}^2}\left(\frac{\psi}{\psi^*}\right)^{-n}\left(\frac{n\epsilon^2}{\psi}+\mu\right)-\frac{2g}{U^*}\left(\frac{U^*}{U_i}\right)^2\frac{a}{g}\right] \tag{14aL}$$

$$\left(\frac{U}{U_i}\right)^2=1+\frac{v_ip_i}{mgl}\left[e^{-h\left(1-\frac{x}{l}\right)}-1\right] \tag{22L}$$

APPENDIX C

AREA AND VOLUME RELATIONS FOR VARIOUS BAG SHAPES

Dimensions used in the expressions given in this appendix are shown in figure 2.

VERTICAL CYLINDER (Fig. 2(a))

$$v=Ax \tag{C1}$$

$$v_i=Al \tag{C2}$$

where A refers to the circular cross-sectional area of the cylinder.

HORIZONTAL CYLINDER (Fig. 2(b))

For inelastic materials the perimeter of the bag cross section is the same before and after deflection, and the length remains constant:

$$P=\pi D$$

$$=2b+\pi x$$

Therefore,

$$b=\frac{\pi D}{2}\left(1-\frac{x}{D}\right)$$

$$A-bL=\frac{\pi DL}{2}\left(1-\frac{x}{D}\right) \tag{C3}$$

$$v_i=\frac{\pi D^2 L}{4} \tag{C4}$$

$$v=L\left(bx+\frac{\pi x^2}{4}\right)$$

$$=\frac{\pi D^2 L}{4}\left[2\frac{x}{D}-\left(\frac{x}{D}\right)^2\right] \tag{C5}$$

HEMISPHERE (Fig. 2(d))

Since the bag is assumed to be inelastic, the radius of the spherical portion of the bag remains unchanged during impact. The bag material in contact with the ground will fold and wrinkle to form an approximately flat surface. The following relations then hold:

$$\left(\frac{b}{2}\right)^2=r^2-x^2$$

$$A=\pi\left(\frac{b}{2}\right)^2=\pi r^2\left[1-\left(\frac{x}{r}\right)^2\right] \tag{C6}$$

$$v=\int_0^x A\,dx$$

$$=\pi r^2\int_0^x\left[1-\left(\frac{x}{r}\right)^2\right]dx$$

$$=\pi r^3\left[\frac{x}{r}-\frac{1}{3}\left(\frac{x}{r}\right)^3\right] \tag{C7}$$

$$v_i=\frac{2}{3}\pi r^3 \tag{C8}$$

SPHERE (Fig. 2(c))

The relations for the sphere can be written directly from those for the hemisphere:

$$A=\frac{\pi D^2}{4}\left[1-\left(\frac{x}{D}\right)^2\right] \tag{C9}$$

$$v=\frac{\pi D^3}{4}\left[\frac{x}{D}-\frac{1}{3}\left(\frac{x}{D}\right)^3\right] \tag{C10}$$

$$v_i=\frac{\pi D^3}{6} \tag{C11}$$

APPENDIX D

GENERALIZED PROCEDURE FOR CALCULATING DECELERATION CHARACTERISTICS WITH GAS BLEED

ANALYSIS

From equations (1), (4), and (10),

$$mU\,dU=\left\{A(p-p_0)-mg\left[1-\left(\frac{U}{U_i}\right)^2\right]\right\}dx \tag{D1}$$

which can be written in the incremental form

$$\Delta U=\frac{\overline{A}p_0\,\Delta x}{m\overline{U}}\left\{\frac{\overline{p}}{p_0}-1-\frac{mg}{\overline{A}p_0}\left[1-\left(\frac{\overline{U}}{U_i}\right)^2\right]\right\} \tag{D2}$$

Since

$$\Delta x=\overline{U}\,\Delta t$$

$$\epsilon=A\mathscr{L}/v_i$$

and

$$\beta=\frac{mg\mathscr{L}}{v_i p_0}$$

equation (D2) can be expressed:

$$\Delta U=\frac{\overline{\epsilon}g\,\Delta t}{\beta}\left\{\frac{\overline{p}}{p_0}-1-\frac{\beta}{\overline{\epsilon}}\left[1-\left(\frac{\overline{U}}{U_i}\right)^2\right]\right\} \tag{D3}$$

Pressure can be expressed in terms of the isentropic relation:

$$p=p_i\left(\frac{\rho}{\rho_i}\right)^\gamma=p_i\lambda^\gamma \tag{D4}$$

By assuming a linear variation of contact area, velocity, and pressure over the increment Δx, equations (D3) and (D4) can be combined to give

$$\Delta U=\frac{(\epsilon_x+\epsilon_{x+\Delta x})\,g\,\Delta t}{4\beta}\left\{\frac{p_i}{p_0}(\lambda_{x+\Delta x}^\gamma+\lambda_x^\gamma)-2-\frac{4\beta}{\epsilon_x+\epsilon_{x+\Delta x}}\left[1-\left(\frac{\overline{U}}{U_i}\right)^2\right]\right\} \tag{D5}$$

For the case where the aerodynamic drag is neglected, the term $(\overline{U}/U_i)^2$ is zero and is omitted from equation (D5).

CALCULATION PROCEDURE

The variation of velocity, decleration, and deceleration onset with stroke can be obtained by the following stepwise procedure:

(1) Assume an arbitrary increment of time Δt. This increment does not have to remain constant during the deceleration process.

(2) Choose or specify the orifice area for the time increment Δt. (This Δt also corresponds to some increment of stroke Δx.) This orifice area can be different at each time increment if desired. For generalized calculations it is convenient to relate this orifice area to the initial volume in ratio form A_n/v_i.

(3) In order to use equation (D5) it is necessary to evaluate ϵ and λ at stations x and $x+\Delta x$. The increment Δx corresponding to time increment Δt is not known accurately because the velocity increment ΔU is not known. As a result, it is necessary to make a first approximation of ϵ_x, λ_x, and $\overline{U}$ to calculate an approximate value of ΔU as follows:

(a) Approximate stroke increment Δx_a:

$$\Delta x_a=U_{x+\Delta x}\,\Delta t$$

$$x_a=(x+\Delta x)-\Delta x_a$$

(b) Values of ϵ:

The value of $x+\Delta x$ is known. For the first increment it is equal to $\mathscr{L}$, and for succeeding increments it is equal to the value of x determined from the preceding increment. Therefore,

$$\epsilon_{x+\Delta x}=f\left(\frac{x+\Delta x}{\mathscr{L}}\right)\ \text{(see table I)}$$

An approximate value of ϵ_{x_a} is obtained based on x_a:

$$\epsilon_{x_a}=f(x_a/\mathscr{D}) \text{ (see table I)}$$

(c) Average velocity $\overline{U}$:

As a first approximation the average velocity is taken as the velocity $U_{x+\Delta x}$.

(d) Density ratio λ:

To calculate the density of the gas it is necessary to know the volume and weight of gas in the bag. The weight is influenced by the bleed, which in turn is influenced by the average pressure within the bag.

The density ratio λ is defined as

$$\lambda=\frac{\rho}{\rho_i}=\frac{W/v_t}{\frac{W_i}{v_i}\psi}$$

The approximate pressure $\overline{p}_a$ is

$$\overline{p}_a=p_i\lambda^{\gamma}_{x+\Delta x}=p_i\left(\frac{W_{x+\Delta x}/v_i}{\frac{W_i}{v_i}\psi_{x+\Delta x}}\right)^{\gamma}$$

$$\frac{W_i}{v_i}=\frac{p_i}{RT_i}$$

(Note: At first increment, $W_{x+\Delta x}=W_i$ and $\psi_{x+\Delta x}=1$.)

$$\frac{\Delta W_a}{v_i}=K\frac{A_n}{v_t}\Delta t\sqrt{\frac{g}{RT_i}}\zeta\Omega$$

where ζ and Ω are obtained from the following equations for $\overline{p}=\overline{p}_a$:

$$\left.\begin{aligned}\zeta&=p_0\sqrt{\frac{2\gamma}{\gamma-1}\left(\frac{p_i}{p_0}\right)^{\frac{\gamma-1}{\gamma}}}\\ \Omega&=\sqrt{\left(\frac{\overline{p}}{p_0}\right)^{\frac{\gamma-1}{\gamma}}-1}\end{aligned}\right\}\begin{array}{l}\text{Subcritical flow where}\\ \dfrac{\overline{p}}{p_0}\le\left(\dfrac{\gamma+1}{2}\right)^{\frac{\gamma}{\gamma-1}}\\ \le 1.893 \text{ for air}\end{array}$$

$$\left.\begin{aligned}\zeta&=p_i\sqrt{\gamma\left(\frac{2}{\gamma+1}\right)^{\frac{\gamma+1}{\gamma-1}}}\\ &=0.685\,p_i \text{ for air}\\ \Omega&=\sqrt{\left(\frac{\overline{p}}{p_i}\right)^{\frac{\gamma+1}{\gamma}}}\end{aligned}\right\}\begin{array}{l}\text{Supercritical flow where}\\ \dfrac{\overline{p}}{p_0}\ge\left(\dfrac{\gamma+1}{2}\right)^{\frac{\gamma}{\gamma-1}}\end{array}$$

The values of ζ and Ω are derived in appendix E.

$$\frac{W_{x_a}}{v_i}=\frac{W_{x+\Delta x}}{v_i}-\frac{\Delta W_a}{v_i}$$

$$\lambda_{x_a}=\frac{\frac{W_{x_a}}{v_t}}{\frac{W_i}{v_t}\psi_{x_a}}$$

(4) Calculate ΔU_a from equation (D5) using values obtained in step (3).

(5) It is now possible to obtain a more accurate value of ΔU, where

$$\overline{U}=U_{x+\Delta x}-\frac{\Delta U_a}{2}$$

$$\Delta x=\overline{U}\,\Delta t$$

$$x=(x+\Delta x)-\Delta x$$

$$\epsilon_x=f(x/\mathscr{D})$$

$$\overline{p}=\frac{p_t}{2}(\lambda^{\gamma}_{x+\Delta x}+\lambda^{\gamma}_{x_a})$$

Values of W_x/v_i and λ_x are calculated in a manner similar to that in step (3), and ΔU is calculated from equation (D5).

(6) A further refined value of x for this increment, which will be $x+\Delta x$ for the next increment, is obtained from

$$x=(x+\Delta x)-\left(U_{x+\Delta x}-\frac{\Delta U}{2}\right)\Delta t$$

where the value of ΔU was obtained in step (5).

(7) The deceleration is calculated from a revised form of equation (12):

$$\left(\frac{a}{g}\right)_x=\frac{\epsilon_x}{\beta}\left(\frac{p_i}{p_0}\lambda^{\gamma}_x-1\right)+\left(\frac{U_x}{U_i}\right)^2-1 \qquad (12d)$$

(8) The deceleration onset rate is calculated from

$$\left(\frac{\dot{a}}{g}\right)_x=\left(\frac{U_x}{U_{x+\Delta x}}\right)\left\{\frac{U_{x+\Delta x}}{\beta\mathscr{D}}\left[\frac{p_{x+\Delta x}}{p_0}\left(\frac{\psi_x}{\psi_{x+\Delta x}}\right)^{-n}\left(\frac{n\epsilon_x^2}{\psi_x}+\mu_x\right)-\mu_x\right]-\frac{2g}{U_{x+\Delta x}}\left(\frac{U_{x+\Delta x}}{U_i}\right)^2\left(\frac{a}{g}\right)_x\right\} \qquad (14b)$$

where the value of n is obtained by combining equations (7) and (D4):

$$n=\frac{\gamma\ln\frac{\rho_x}{\rho_{x+\Delta x}}}{\ln\frac{v_{x+\Delta x}}{v_x}}$$

(9) This calculation procedure is continued over succeeding increments of Δx until the velocity becomes zero or the bag is deflated.

APPENDIX E

DERIVATION OF EQUATIONS FOR FLOW OF GAS THROUGH FLOW NOZZLE

SUBCRITICAL FLOW

The flow rate can be expressed

$$\dot{W}=KA_n\rho_t u_t$$
$$=KA_n p_t M\sqrt{\gamma g/RT_t} \qquad \text{(E1)}$$

Substitution of isentropic relations for Mach number, pressure, and temperature results in

$$\dot{W}=KA_n p_t\sqrt{\frac{2g}{RT}\left(\frac{\gamma}{\gamma-1}\right)\left(\frac{p}{p_t}\right)^{\frac{\gamma-1}{\gamma}}\left[\left(\frac{p}{p_t}\right)^{\frac{\gamma-1}{\gamma}}-1\right]} \qquad \text{(E2)}$$

The gas temperature in the bag is

$$T=T_i\left(\frac{p}{p_i}\right)^{\frac{\gamma-1}{\gamma}}$$

and for subsonic flow

$$p_t=p_0$$

so that equation (E2) becomes

$$\dot{W}=KA_n p_0\sqrt{\left(\frac{2g}{RT_i}\right)\left(\frac{\gamma}{\gamma-1}\right)\left(\frac{p_i}{p_0}\right)^{\frac{\gamma-1}{\gamma}}\left[\left(\frac{p}{p_0}\right)^{\frac{\gamma-1}{\gamma}}-1\right]} \qquad \text{(E3)}$$

The weight loss over time increment Δt is expressed by

$$\Delta W=\dot{W}\,\Delta t=KA_n\,\Delta t\sqrt{\frac{g}{RT_i}}\,\zeta\Omega \qquad \text{(E4)}$$

where

$$\zeta=p_0\sqrt{\frac{2\gamma}{\gamma-1}\left(\frac{p_i}{p_0}\right)^{\frac{\gamma-1}{\gamma}}} \qquad \text{(E5)}$$

$$\Omega=\sqrt{\left(\frac{p}{p_0}\right)^{\frac{\gamma-1}{\gamma}}-1} \qquad \text{(E6)}$$

SUPERCRITICAL FLOW

For supercritical flow the velocity will be sonic at the throat of the flow nozzle. Then,

$$\dot{W}=K\rho_t A_n u_t$$
$$=KA_n p_t\sqrt{\frac{\gamma g}{RT_t}} \qquad \text{(E7)}$$

Since

$$p_t=\frac{p}{\left(\frac{\gamma+1}{2}\right)^{\frac{\gamma}{\gamma-1}}}$$

and

$$T_t=T_i\left(\frac{p}{p_i}\frac{p_t}{p}\right)^{\frac{\gamma-1}{\gamma}}$$

then

$$\dot{W}=KA_n\left(\frac{2}{\gamma+1}\right)^{\frac{\gamma+1}{2(\gamma-1)}}p_i\left(\frac{p}{p_i}\right)^{\frac{\gamma+1}{2\gamma}}\sqrt{\frac{\gamma g}{RT_i}} \qquad \text{(E8)}$$

The weight loss over the time increment Δt is

$$W=\dot{W}\,\Delta t=KA_n\,\Delta t\sqrt{\frac{g}{RT_i}}\,\zeta\Omega \qquad \text{(E9)}$$

where for the supercritical flow

$$\zeta=p_i\sqrt{\gamma\left(\frac{2}{\gamma+1}\right)^{\frac{\gamma+1}{\gamma-1}}} \qquad \text{(E10)}$$

$$\Omega=\left(\frac{p}{p_i}\right)^{\frac{\gamma+1}{2\gamma}} \qquad \text{(E11)}$$

REFERENCES

1. Vaughan, Victor L., Jr.: Water-Landing Impact Accelerations for Three Models of Reentry Capsules. NASA TN D–145, 1959.
2. Ali, Ahmin, and Benson, Leonard R.: Cushioning for Air Drop. Pt. IX –Bibliography of Literature Pertaining to the Absorption of Impact Energy. Structural Mechanics Res. Lab., The Univ. of Texas, June 9, 1957. (Contract DA 19–129 QM–150.)
3. Karnes, Charles H., Turnbow, James W., Ripperger, E. A., and Thompson, J. Neils: High-Velocity Impact Cushioning. Pt. V –Energy-Absorption Characteristics of Paper Honeycomb. Structural Mechanics Res. Lab., The Univ. of Texas, May 25, 1959. (Contract DA 19–129 QM 817.)
4. Anon.: Decelerator Bag Study –Item 1–A. The Goodyear Tire & Rubber Co., May 15, 1956. (Contract AF–33(600)30825.)
5. Tomesak, S. L., Duvall, W. C., and Mettler, C. A.: Decelerator Bag Study – Item 1–B. The Goodyear Tire & Rubber Co., Dec. 1957. (Contract AF–33(600)30825.)
6. Anon.: Decelerator Bag Study –Item 2–A Supplement. The Goodyear Tire & Rubber Co., Aug. 27, 1958. (Contract AF 33(600)30825.)
7. Matlock, Hudson, and Thompson, J. Neils: High-Velocity Impact Cushioning. Pt. III –Preliminary Tests on a Nonpressurized Air Bag. Structural Mechanics Res. Lab., The Univ. of Texas, Oct. 15, 1957. (Contract DA 19–129–QM–817.)
8. Idomir, Kenneth: TM–76 Mace Landing Mat Design. Aero/Space Eng., vol. 19, no. 2, Feb. 1960, pp. 28–34.
9. Martin, E. D., and Howe, J. T.: An Analysis of the Impact Motion of an Inflated Sphere Landing Vehicle. NASA TN D–314, 1960.
10. Howe, John T., and Martin, E. D.: Gas Dynamics of an Inflated Sphere Striking a Surface. NASA TN D–315, 1960.
11. Eiband, A. Martin: Human Tolerance to Rapidly Applied Accelerations: A Summary of the Literature. NASA MEMO 5–19–59E, 1959.

TABLE I.—RELATIONS FOR VARIOUS BAG SHAPES USED IN ANALYSIS

Function	Type of bag			
	Vertical cylinder	Horizontal cylinder	Sphere	Hemisphere
$\mathscr{D}$	l	D	D	r
A	A	$\frac{\pi DL}{2}\left(1-\frac{x}{D}\right)$	$\frac{\pi D^2}{4}\left[1-\left(\frac{x}{D}\right)^2\right]$	$\pi r^2\left[1-\left(\frac{x}{r}\right)^2\right]$
v_i	Al	$\frac{\pi D^2 L}{4}$	$\frac{\pi D^3}{6}$	$\frac{2}{3}\pi r^3$
v	Ax	$\frac{\pi D^2 L}{4}\left[2\left(\frac{x}{D}\right)-\left(\frac{x}{D}\right)^2\right]$	$\frac{\pi D^3}{4}\left[\frac{x}{D}-\frac{1}{3}\left(\frac{x}{D}\right)^3\right]$	$\pi r^3\left[\frac{x}{r}-\frac{1}{3}\left(\frac{x}{r}\right)^3\right]$
$\psi=\frac{v}{v_i}$	$\frac{x}{l}$	$2\frac{x}{D}-\left(\frac{x}{D}\right)^2$	$\frac{3}{2}\frac{x}{D}-\frac{1}{2}\left(\frac{x}{D}\right)^3$	$\frac{3}{2}\frac{x}{r}-\frac{1}{2}\left(\frac{x}{r}\right)^3$
$\mathrm{d}\psi$	$\frac{\mathrm{d}x}{l}$	$\frac{2}{D}\left(1-\frac{x}{D}\right)\mathrm{d}x$	$\frac{3}{2D}\left[1-\left(\frac{x}{D}\right)^2\right]\mathrm{d}x$	$\frac{2}{3r}\left[1-\left(\frac{x}{r}\right)^2\right]\mathrm{d}x$
$v_i\,\mathrm{d}\psi$	$A\,\mathrm{d}x$	$\frac{\pi DL}{2}\left(1-\frac{x}{D}\right)\mathrm{d}x$	$\frac{\pi D^2}{4}\left[1-\left(\frac{x}{D}\right)^2\right]\mathrm{d}x$	$\pi r^2\left[1-\left(\frac{x}{r}\right)^2\right]\mathrm{d}x$
β	$\frac{mgl}{v_i p_0}$	$\frac{mgD}{v_i p_0}$	$\frac{mgD}{v_i p_0}$	$\frac{mgr}{v_i p_0}$
$\epsilon=\frac{A\mathscr{D}}{v_i}$	1	$2\left(1-\frac{x}{D}\right)$	$\frac{3}{2}\left[1-\left(\frac{x}{D}\right)^2\right]$	$\frac{3}{2}\left[1-\left(\frac{x}{r}\right)^2\right]$
μ	0	2	$3\frac{x}{D}$	$3\frac{x}{r}$

TABLE II.—MAXIMUM DECELERATION ONSET RATES

Bag geometry [a]	Reference figure	U_i, ft/sec	p_i/p_0	m/v_i, $\frac{\text{lb-sec}^2}{\text{ft}^4}$	$\mathscr{D}$, ft	$(\dot{a}/g)_{max}$, g's/sec
VC	4	30	1.0	2	2	1055
		30	1.0	2	4	284
	5	30	1.0	2	3	488
		↓	1.2	↓	↓	[b] 484
		↓	1.4	↓	↓	[b] 340
HC	5	30	1.0	2	3	1259
		↓	1.2	↓	↓	926
		↓	1.4	↓	↓	735
S or H	5	30	1.0	2	3	1018
		↓	1.2	↓	↓	763
		↓	1.4	↓	↓	638
VC	6(a)	20	1.0	1	2	632
		↓	↓	2	↓	418
		↓	↓	3	↓	361
		↓	↓	4	↓	345
		30	↓	1	↓	[c] 1308
		↓	↓	2	↓	1055
		↓	↓	3	↓	1088
		↓	↓	4	↓	1193
		40	↓	1	↓	[c] 2501
		↓	↓	2	↓	[c] 2556
		↓	↓	3	↓	[c] 3030
		↓	↓	4	↓	[c] 3771
	6(b)	20	1.0	1	3	281
		↓	↓	2	↓	188
		↓	↓	3	↓	166
		↓	↓	4	↓	163
		30	↓	1	↓	588
		↓	↓	2	↓	488
		↓	↓	3	↓	510
		↓	↓	4	↓	570
		40	↓	1	↓	1123
		↓	↓	2	↓	1174
		↓	↓	3	↓	[c] 1397
		↓	↓	4	↓	[c] 1751
	6(c)	20	1.0	1	4	157
		↓	↓	2	↓	107
		↓	↓	3	↓	97
		↓	↓	4	↓	96
VC	6(c)	30	1.0	1	4	333
		↓	↓	2	↓	284
		↓	↓	3	↓	302
		↓	↓	4	↓	341
		40	↓	1	↓	643
		↓	↓	2	↓	686
		↓	↓	3	↓	834
		↓	↓	4	↓	1066
VC	7	30	1.0	2	3	489
HC	7	30	1.0	2	3	[c] 1259
S or H	7	30	1.0	2	3	1081
VC	8	30	2.0	2	3	[c] ∞
HC	8	30	2.0	2	3	218
S or H	8	30	2.0	2	3	309
VC	9	30	1.0	2	3	396
HC	9	30	1.0	2	3	698
S or H	9	30	1.0	2	3	631
VC	10	30	1.0	2	3	488
		↓	↓	2	↓	[d] 828
		↓	↓	4	↓	[d] 808
	11	30	1.0	2	3	488
		↓	↓	4	↓	[d] 414
		↓	↓	6	↓	[d] 485
VC–1	12(a)	30	1.0	2	3	683
–2		↓	↓	↓	↓	596
–4		↓	↓	↓	↓	300
VC–1	12(b)	30	1.0	2	3	635
–2		↓	↓	↓	↓	518
–4		↓	↓	↓	↓	380

[a] Symbols for bag geometry: VC, vertical cylinder; HC, horizontal cylinder; S, sphere; H, hemisphere; 1, 2, 4, relative orifice size.
[b] After initial shock at impact.
[c] Deceleration onset probably too high for humans (ref. 11).
[d] After initial 10-g deceleration.

U.S. GOVERNMENT PRINTING OFFICE: 1961